



Image-based modelling of problems in cell motility

Till Bretschneider
Department of Computer Science
member of SBIDER and CMCB
University of Warwick

SFB 1294 Golm, 9. November 2018

Cell motility

Two principal forms of cell migration exist: mesenchymal and amoeboid.
Many cell types can switch between the two forms (plasticity)

	Mesenchymal	Amoeboid
prototype	fibroblasts	macrophages
cell shape	elongated	round
cell-matrix interaction	proteolysis	displacement/squeezing through
substrate attachment	integrin based adhesion	mostly unspecific
velocity	~ 10 $\mu\text{m}/\text{h}$	~ 10 $\mu\text{m}/\text{min}$
propulsion	lamellipodia	pseudopodia/blebs, high myosin-II dependent contractility

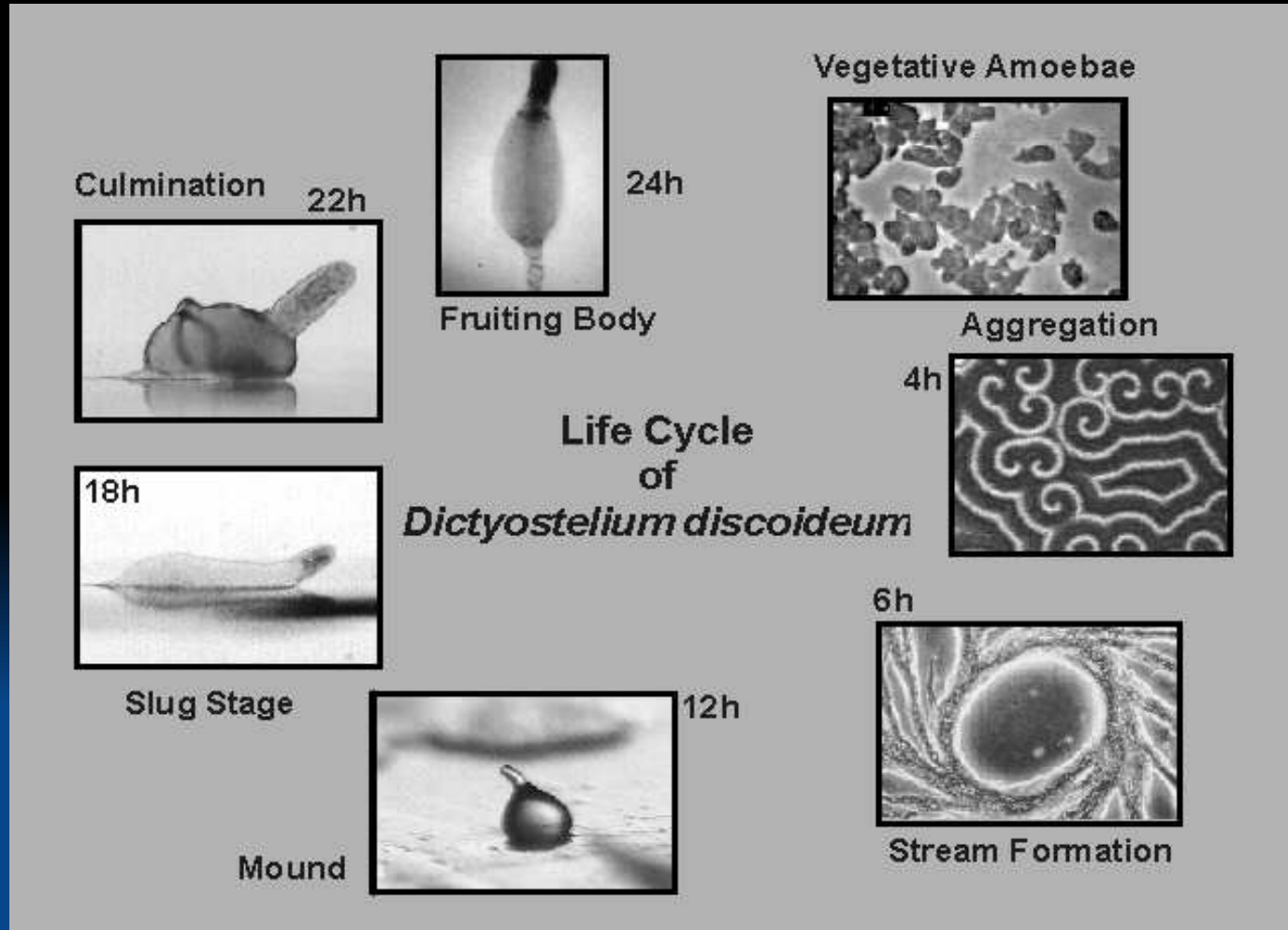
(adapted from Pankova et al., Cell. Mol. Life Sci. 2010, 67:63–71)

examples of amoeboid motility

- immune system
- fast tumour cell invasion
- primordial germ cell migration
- motility of protozoan pathogens (*Entamoeba histolytica*)
- Model system: *Dictyostelium discoideum*

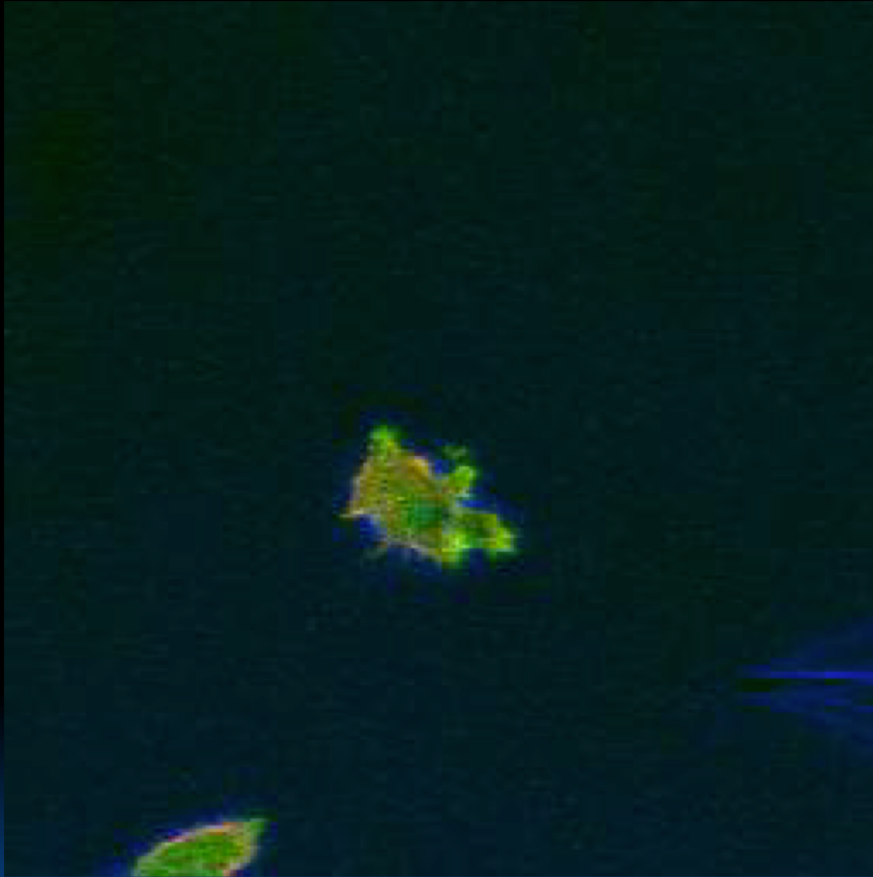
Dictyostelium discoideum

Relay of cAMP pulses by cells results in spreading of cAMP waves through a population of starved cells. Cells aggregate due to directed motion (chemotaxis) towards a cAMP source.



Dictyostelium Chemotaxis:

Actin-Assembly at the Front and Myosin-II Recruitment to the Tail



Green: Polymerized actin

Red: Myosin II

Frame interval: 5 seconds

movie by J. Dalous

Main Questions:

How can we quantify spatio-temporal patterns in moving cells?

How can we relate these to movement?

Can we develop predictive mathematical models for cell movement?

Outline

- Analysing dynamic fluorescence distributions in the cortex of moving cells (QuimP software)
- Parameterization of different models for cell reorientation
- The role of membrane tension in cellular blebbing
- 3D light sheet imaging of cell surface dynamics during macro-pinocytosis & new computational tools

Baniukiewicz P, Collier S, Bretschneider T. QuimP – Analyzing transmembrane signalling in highly deformable cells. *Bioinformatics*, 34(15), 2695–7, 2018.

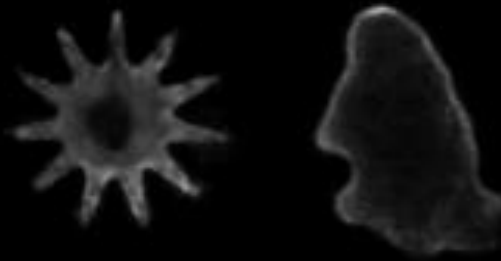
Lockley R, Ladds G, Bretschneider T. Image based validation of dynamical models for cell reorientation. *Cytometry A*, 87(6):471-80, 2015

Zatulovskiy E, Tyson R, Bretschneider T, Kay RR. Bleb-driven chemotaxis of Dictyostelium cells. *J Cell Biol*. 204(6):1027-44, 2014.

Tyson RA, Zatulovskiy E, Kay RR, Bretschneider T. How blebs and pseudopods cooperate during chemotaxis. *PNAS* 111(32):11703-8. 2014

Collier S, Paschke P, Kay RR, Bretschneider T. Image based modelling of bleb site selection. *Scientific Reports*, 7, 6692, 2017

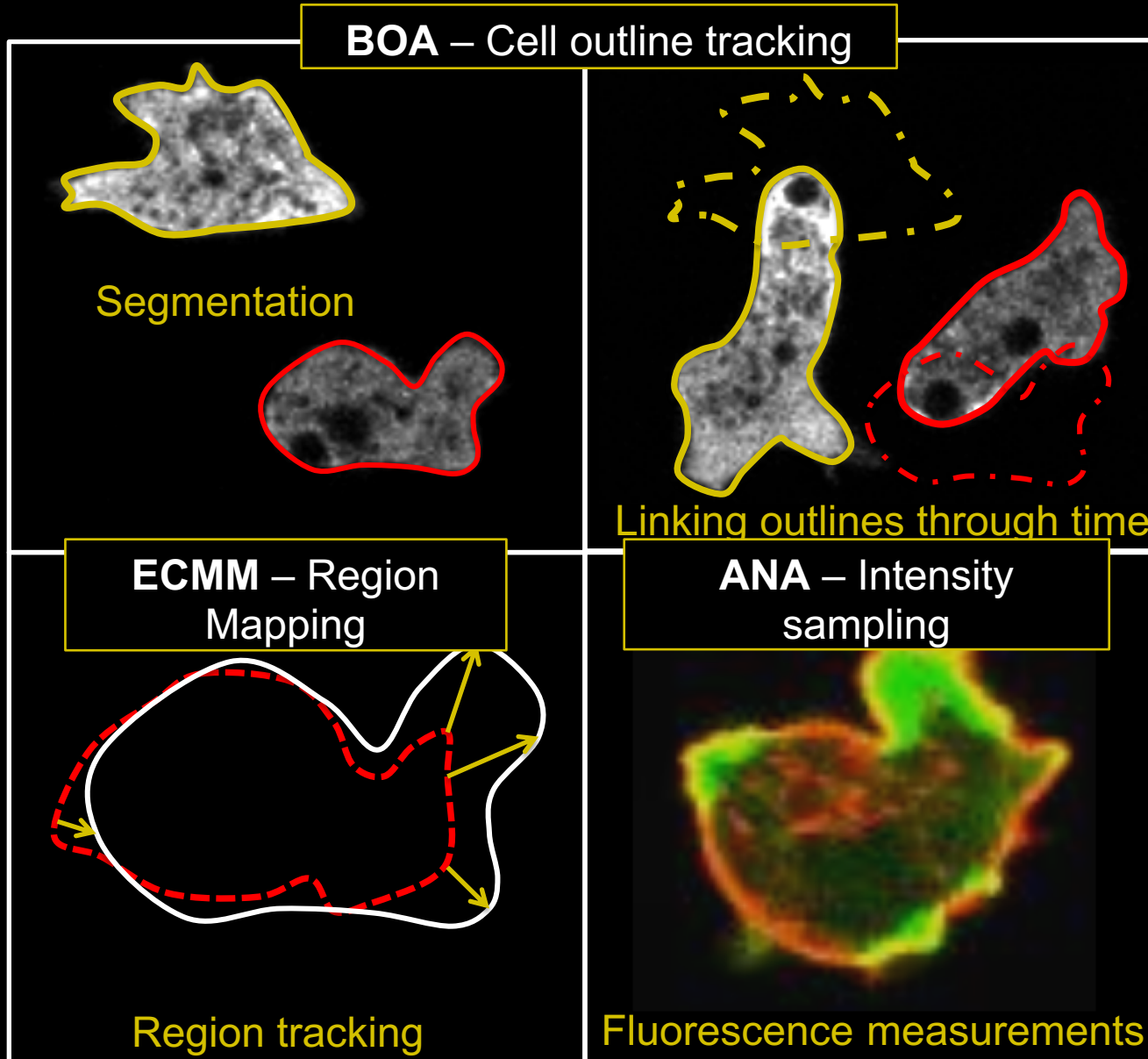
Baniukiewicz P, Collier S, Bretschneider T. Generative adversarial networks for augmenting training data of microscopic cell images. Submitted to ISBI 2019.



Outline

- **Analysing dynamic fluorescence distributions in the cortex of moving cells (QuimP software)**
- Parameterization of different models for cell reorientation
- The role of membrane tension in cellular blebbing
- 3D light sheet imaging of cell surface dynamics during macro-pinocytosis & new computational tools

QuimP: ImageJ plugins for quantifying cellular morphodynamics



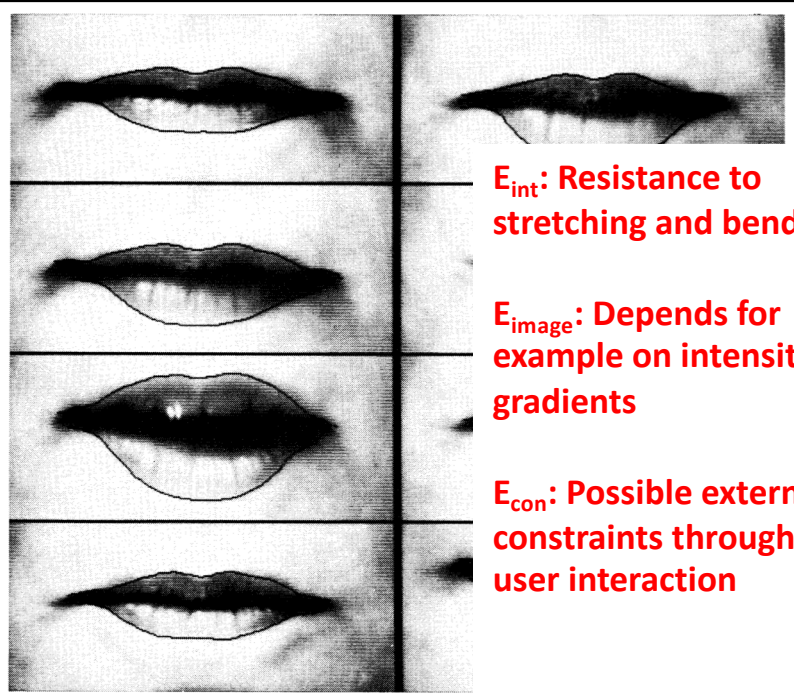
Cell segmentation

Pixel based methods: Thresholding, clustering based, entropy based, region growing/watershed/graph based/anisotropic diffusion, ...

Contour based methods (active contours/level set methods, 1980s)

Convolutional Neural Networks/Deep learning (2010s)

QuimP's main/original segmentation method is based on active contours



E_{int} : Resistance to stretching and bending

E_{image} : Depends for example on intensity gradients

E_{con} : Possible external constraints through user interaction

International Journal of Computer Vision, 321-331 (1988)
© 1987 Kluwer Academic Publishers, Boston, Manufactured in The Netherlands

Snakes: Active Contour Models

ICHAEL KASS, ANDREW WITKIN, and DEMETRI TERZOPOULOS
humberger Palo Alto Research, 3340 Hillview Ave., Palo Alto, CA 94304

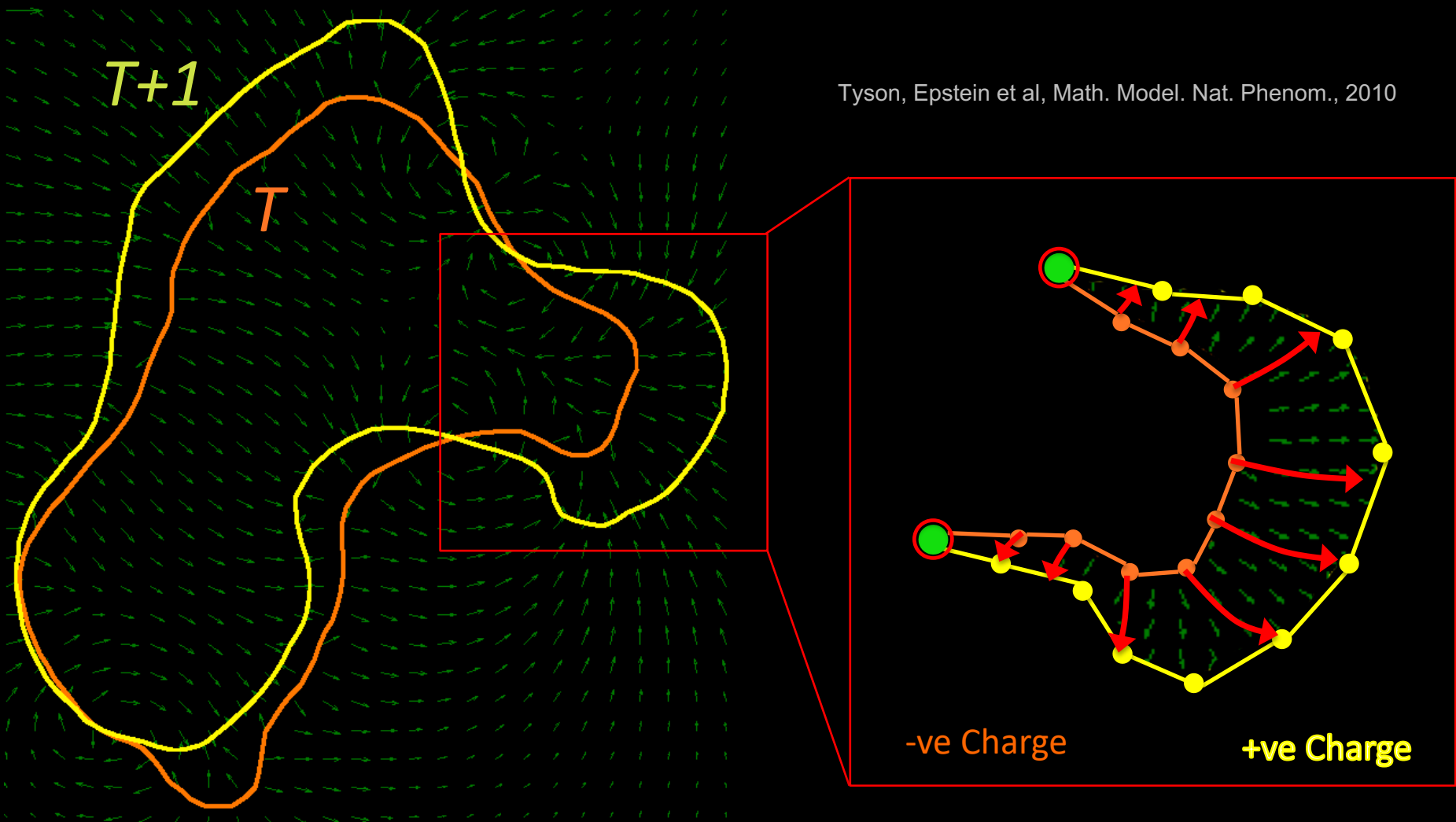
$$\begin{aligned} E_{\text{snake}}^* &= \int_0^1 E_{\text{snake}}(\mathbf{v}(s)) ds \\ &= \int_0^1 E_{\text{int}}(\mathbf{v}(s)) + E_{\text{image}}(\mathbf{v}(s)) \\ &\quad + E_{\text{con}}(\mathbf{v}(s)) ds \end{aligned}$$

8. Selected frames from a 2-second video sequence show snakes used for motion tracking. After being initialized to the speaker's lips in the first frame, the snakes automatically track the lip movements with high accuracy.

> 9000 citations (Scopus)

Electrostatic Contour Mapping Method (ECMM)

Tyson, Epstein et al, Math. Model. Nat. Phenom., 2010



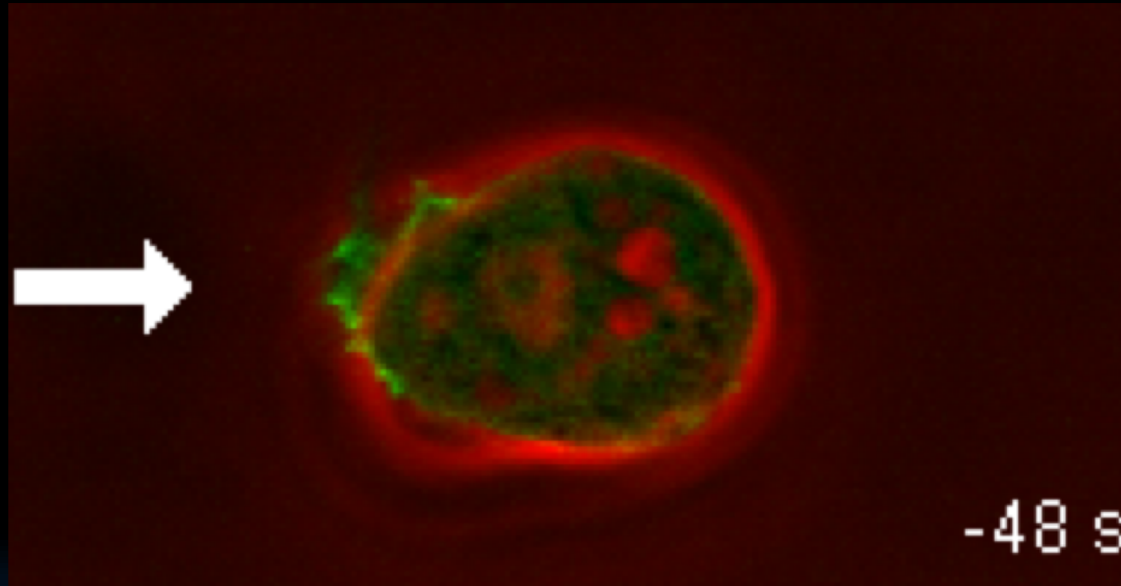
Field lines never cross!

ECMM provides a unique solution, which minimises the total path integral, ie the energy needed to match two cell outlines at subsequent time points

Outline

- Analysing dynamic fluorescence distributions in the cortex of moving cells (QuimP software)
- **Parameterization of different models for cell reorientation**
- The role of membrane tension in cellular blebbing
- 3D light sheet imaging of cell surface dynamics during macro-pinocytosis & new computational tools

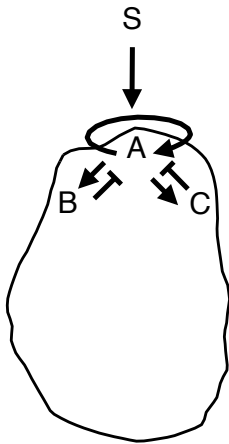
Modelling cell reorientation: Response of *Dictyostelium* to shear flow reversals



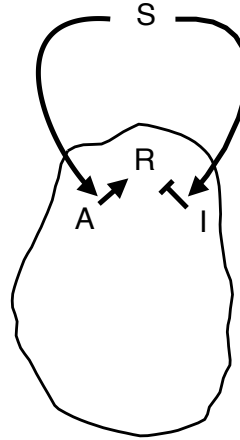
green: Actin label
red: phase contrast

Reaction-diffusion models for cell front activation

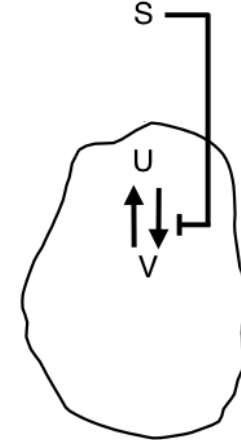
Meinhardt



Levchenko/Iglesias



Otsuji



$$\frac{\partial A}{\partial t} = \frac{sr_a(\frac{A^2}{B} + b_a)}{(s_c + C)(1 + s_a A^2)} - r_a A + D_A \frac{\partial^2 A}{\partial x^2}$$

$$\frac{dB}{dt} = r_b \sum_n \frac{A}{n} - r_b B$$

$$\frac{\partial C}{\partial t} = b_c A - r_c C + D_C \frac{\partial^2 C}{\partial x^2}$$

$$\frac{\partial A}{\partial t} = k_{AS} - k_{-A}A$$

$$\frac{\partial I}{\partial t} = k_{IS} - k_{-I}I + D_I \frac{\partial^2 I}{\partial x^2}$$

$$\frac{\partial R}{\partial t} = k_{RA}(R_T - R) - k_{-R}IR$$

$$\frac{\partial U}{\partial t} = a_1 \left[V - \frac{U + V}{(a_2 s(U + V) + 1)^2} \right] + D_U \frac{\partial^2 U}{\partial x^2}$$

$$\frac{\partial V}{\partial t} = a_1 \left[\frac{U + V}{(a_2 s(U + V) + 1)^2} - V \right] + D_V \frac{\partial^2 V}{\partial x^2}$$

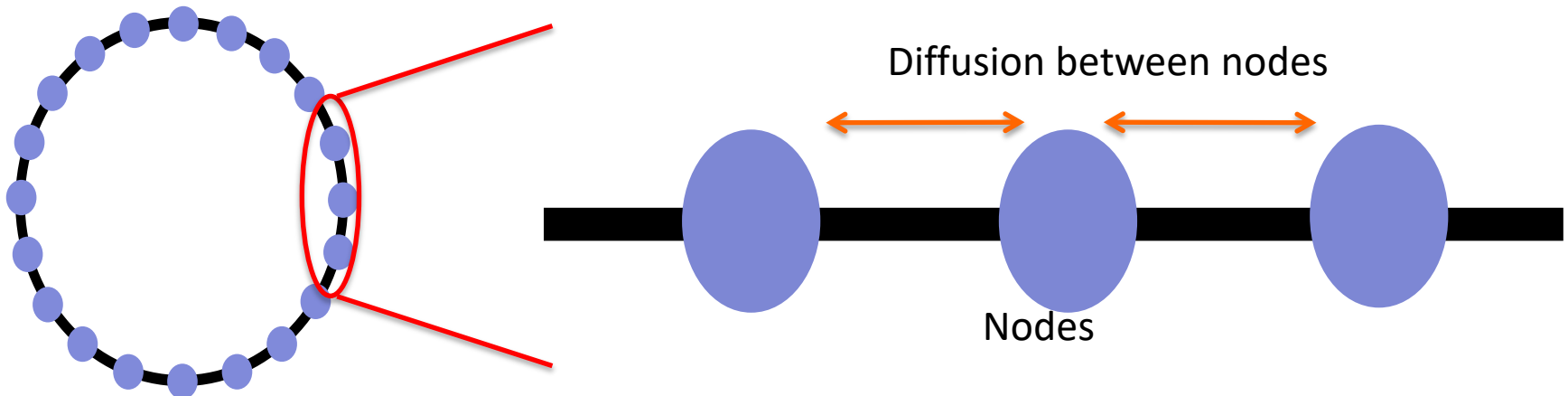
external signal $s = (1 + dy \cos(2\pi x))$

Model Fitting

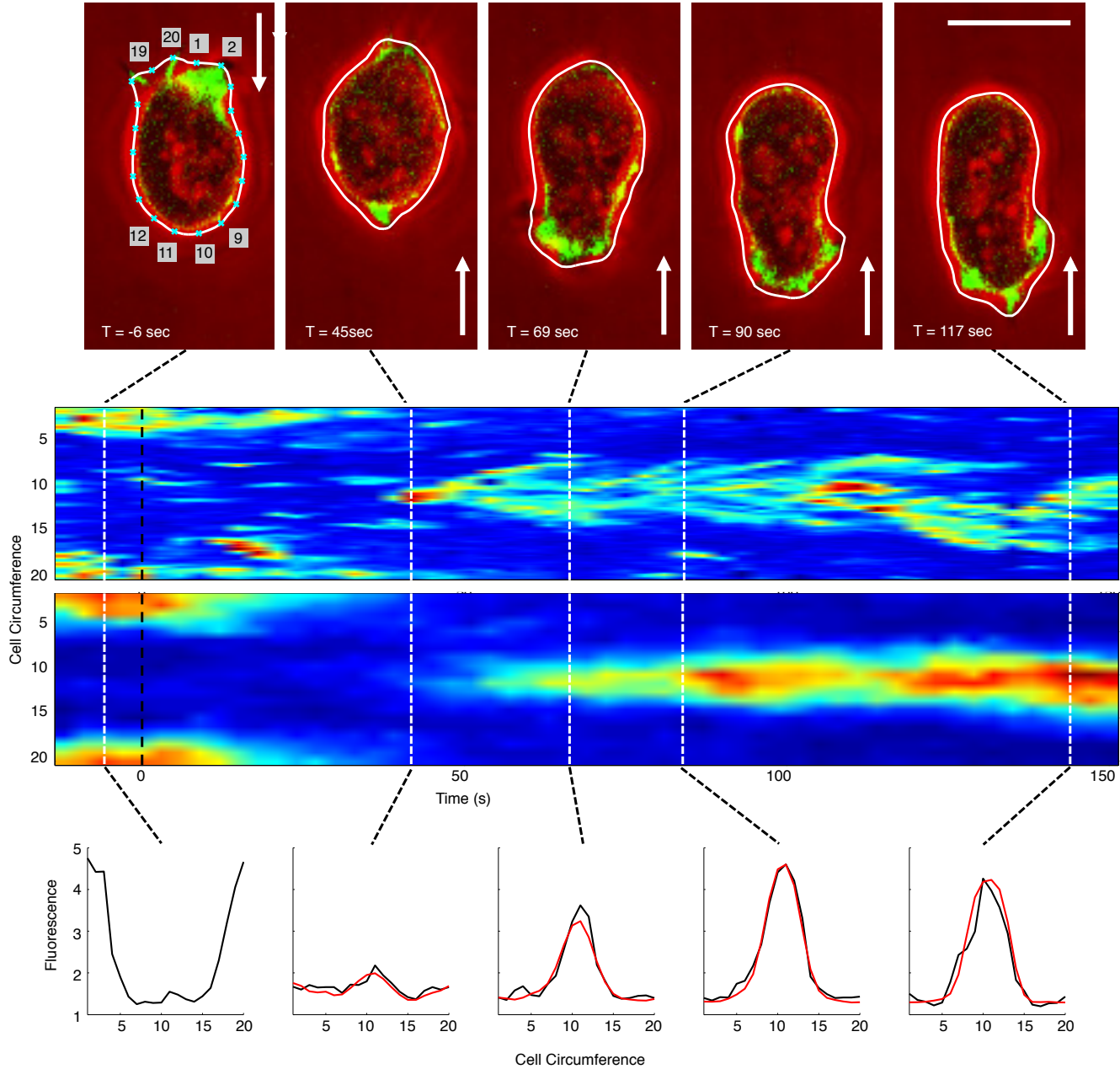
- Experimental data: actin fluorescence sampled at P=20 points in the cell cortex is taken as readout of the activator
- 1D PDE model on a closed circle (periodic boundary conditions)
- Finite differences for approximating diffusion

$$\partial^2 C_i / \partial x^2 \approx (C_{i-1} - 2C_i + C_{i+1}) / (\Delta x)^2$$

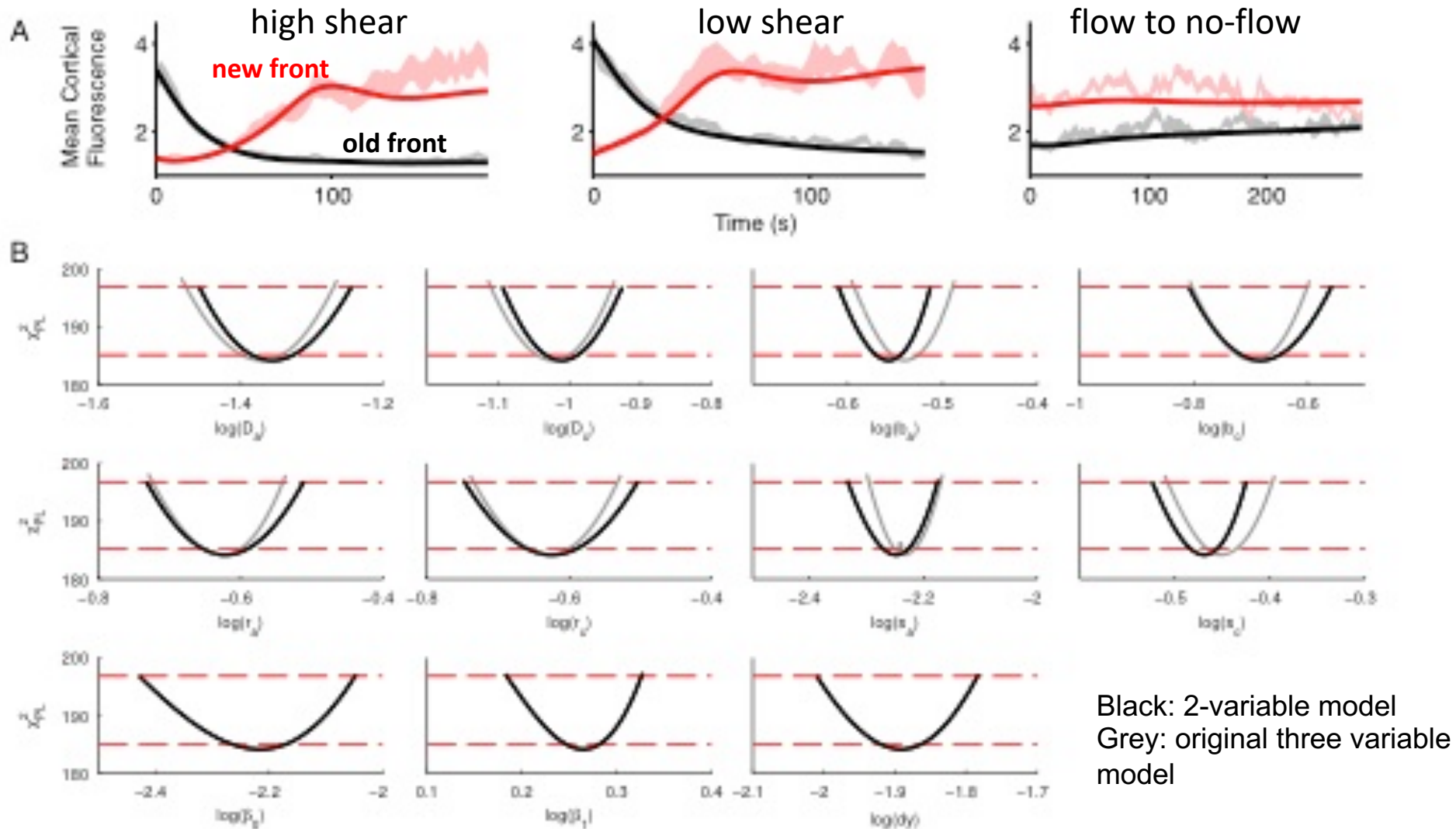
- N-variable PDE problem is expressed as system of PxN ODEs
- Standard ODE solvers (RK45) and NLLS methods for fitting can be used
- Implementation in PottersWheel (MATLAB)



Fitting models to averaged time course data



A reduced two-variable Meinhardt model is fully identifiable



Identifiability: for each of the eleven parameters chi-squared, the quadratic error of the fit, has a clear minimum; Dashed red lines: pointwise and simultaneous likelihood-based confidence intervals $\{\theta \mid \chi^2(\theta) - \chi^2(\hat{\theta}) < \Delta\alpha\}$ with $\Delta\alpha = \chi^2(\alpha, df)$, $\alpha = 68\%$

Reducing the Meinhardt model

- Inhibitor B almost stays constant
- replace it by $B(P)=1 + \beta_0(P^2 + \beta_1P)$ where P is the pressure in Pascal
- $dy(P=0) = 0$, and $dy(P) = \text{const}$

$$\frac{\partial A}{\partial t} = \frac{sr_a(\frac{A^2}{B} + b_a)}{(s_c + C)(1 + s_a A^2)} - r_a A + D_A \frac{\partial^2 A}{\partial x^2}$$

$$\frac{dB}{dt} = r_b \sum_n \frac{A}{n} - r_b B$$

$$\frac{\partial C}{\partial t} = b_c A - r_c C + D_C \frac{\partial^2 C}{\partial x^2}$$

$$s = (1 + dy \cos(2\pi x))$$

original

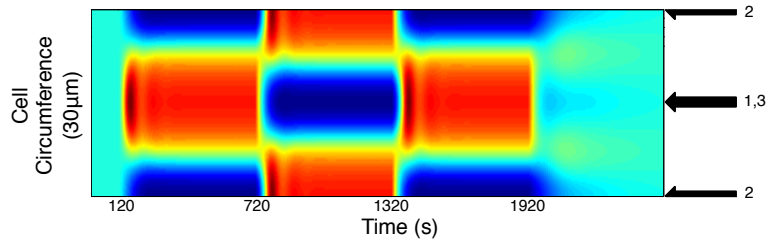
$$\frac{\partial A}{\partial t} = \frac{sr_a(\frac{A^2}{B(P)} + b_a)}{(s_c + C)(1 + s_a A^2)} - r_a A + D_A \frac{\partial^2 A}{\partial x^2}$$

$$\frac{\partial C}{\partial t} = b_c A - r_c C + D_C \frac{\partial^2 C}{\partial x^2}$$

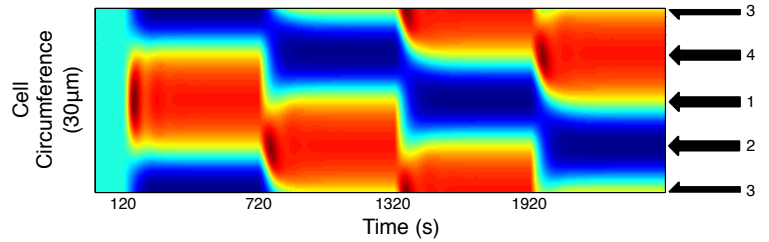
$$s = (1 + dy(P) \cos(2\pi x))$$

modified

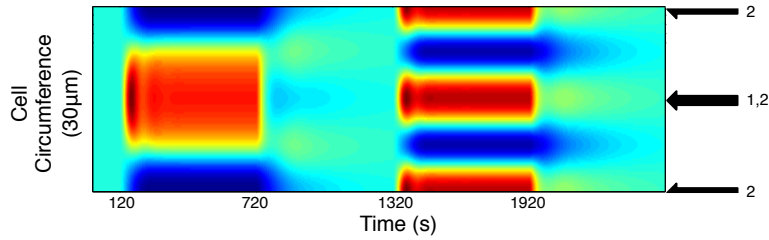
Simulations of hallmark chemotaxis experiments



polarity inversion



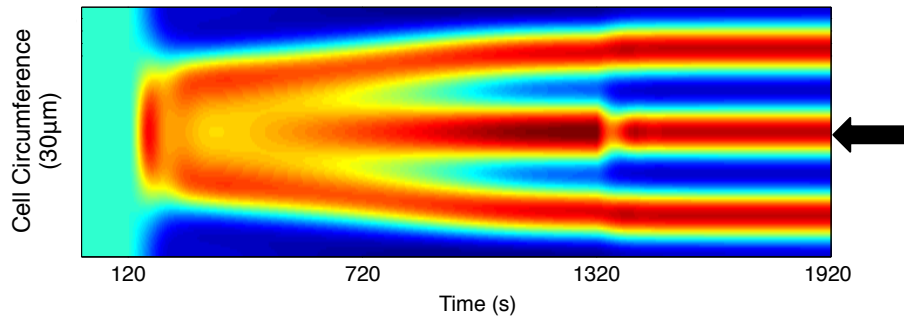
response to gradually moving signal



response to two signals on opposite sides

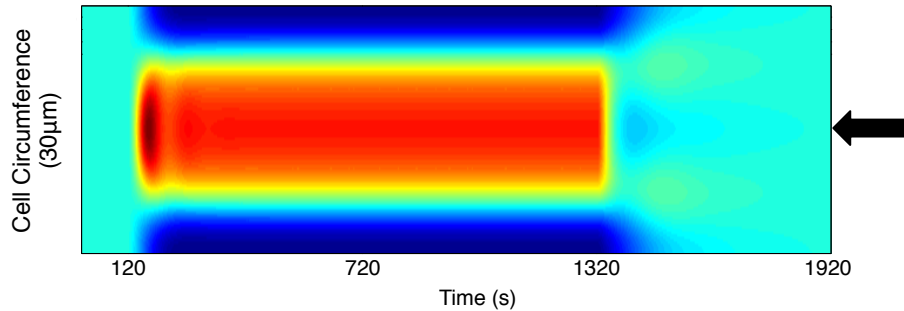
Predicting long time behaviour

A Fitted Model Parameters



Parameters derived from previous experiments result in front splitting

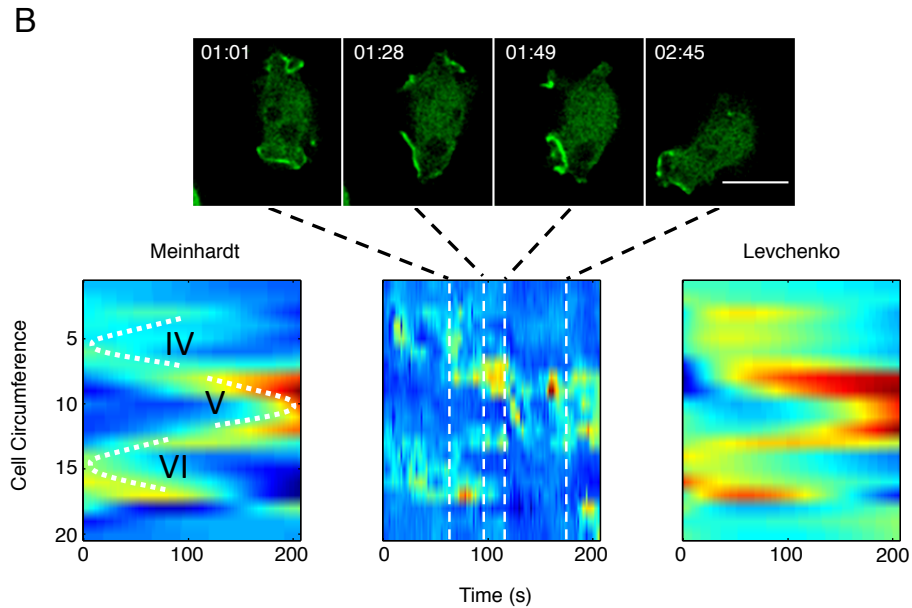
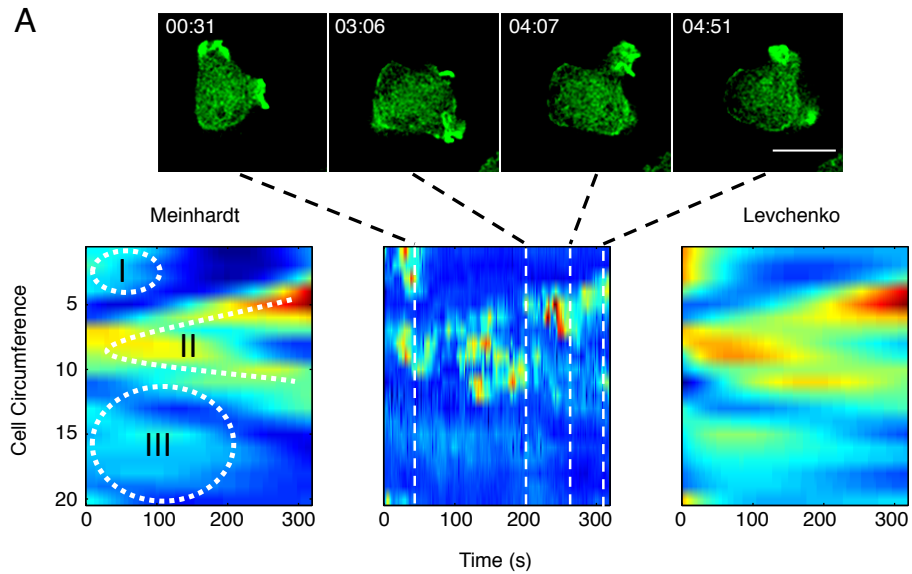
B Fitted Model Parameters with Decreased D_C



Front splitting can be abolished by reducing D_C (minus 35%), which changes previous fits only marginally

signal present (1Pa)

Fitting spontaneous movement of single cells



Switching from a single front to multiple fronts (random motility) entails shutting down inhibitor diffusion in the model

Original Meinhardt 3-variable		Meinhardt 2-variable (identifiable)		Meinhardt 2-variable Single stable front		Meinhardt 2-variable Random motility	
$D_A (\mu\text{m}^2\text{s}^{-1})$	9.61×10^{-2}	$D_A (\mu\text{m}^2\text{s}^{-1})$	9.95×10^{-2}	$D_A (\mu\text{m}^2\text{s}^{-1})$	=	$D_A (\mu\text{m}^2\text{s}^{-1})$	5.20×10^{-3}
$D_C (\mu\text{m}^2\text{s}^{-1})$	2.13×10^{-1}	$D_C (\mu\text{m}^2\text{s}^{-1})$	2.20×10^{-1}	$D_C (\mu\text{m}^2\text{s}^{-1})$	1.43×10^{-1}	$D_C (\mu\text{m}^2\text{s}^{-1})$	3.31×10^{-8}
b_a	2.88×10^{-1}	b_a	2.78×10^{-1}	b_a	=	b_a	1.44×10^{-1}
$b_c (s^{-1})$	2.02×10^{-1}	$b_c (s^{-1})$	2.08×10^{-1}	$b_c (s^{-1})$	=	$b_c (s^{-1})$	5.64×10^{-2}
$r_a (s^{-1})$	2.37×10^{-1}	$r_a (s^{-1})$	2.39×10^{-1}	$r_a (s^{-1})$	=	$r_a (s^{-1})$	9.47×10^{-2}
$r_c (s^{-1})$	2.35×10^{-1}	$r_c (s^{-1})$	2.38×10^{-1}	$r_c (s^{-1})$	=	$r_c (s^{-1})$	6.55×10^{-2}
s_a	5.83×10^{-3}	s_a	5.65×10^{-3}	s_a	=	s_a	3.05×10^{-3}
s_c	3.53×10^{-1}	s_c	3.40×10^{-1}	s_c	=	s_c	2.79×10^{-1}
$r_b (s^{-1})$	[practically non. ident.]						
		$\beta_0 (\text{Pa}^{-2})$	6.07×10^{-3}	$\beta_0 (\text{Pa}^{-2})$	=		
dy_{low}	1.31×10^{-2}	$\beta_1 (\text{Pa})$	1.84	$\beta_1 (\text{Pa})$	=		
dy_{high}	1.28×10^{-2}	dy	1.28×10^{-2}	dy	=		

Mechanotaxis (here): Diffusion of activator: $0.1 \mu\text{m}^2\text{sec}^{-1}$

Diffusion of phospholipids (Pip2/PIP3) in membrane (Ueda, bioRxiv, 2018): $0.2 \mu\text{m}^2\text{sec}^{-1}$

Diffusion of cAMP receptor (Ueda et al., Science 2001): $0.02 \mu\text{m}^2\text{sec}^{-1}$

Conclusions Reorientation

- Models by Meinhardt and Levchenko fit complex patterns observed in reorientation experiments and spontaneous cell movements
- A reduced 2-variable version of the Meinhardt model is fully identifiable.
- Differences between cells producing one dominant or multiple competing fronts can be explained by reduced activator and inhibitor diffusion.

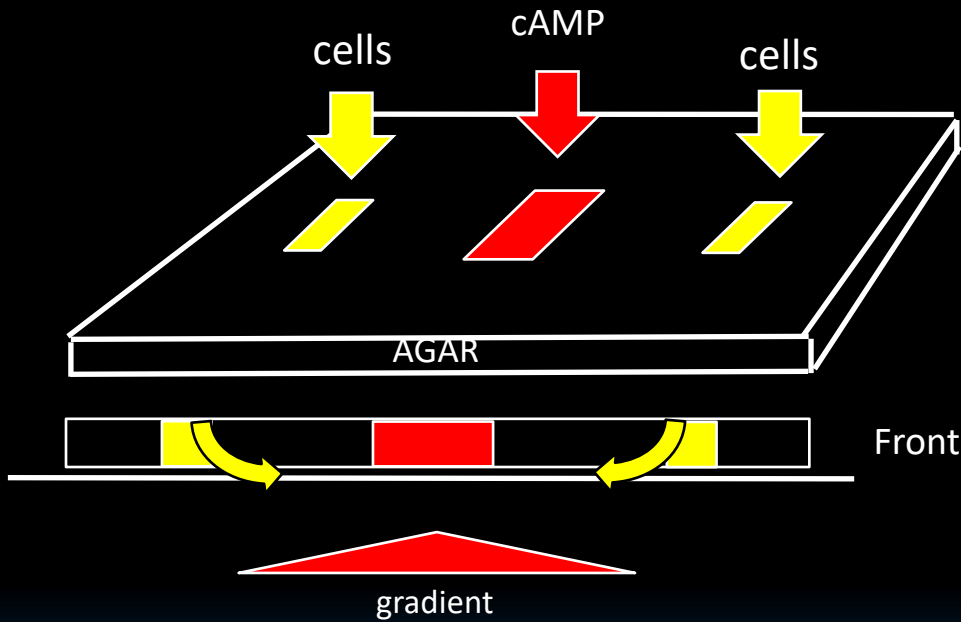
Outline

- Analysing dynamic fluorescence distributions in the cortex of moving cells (QuimP software)
- Parameterization of different models for cell reorientation
- **The role of membrane tension in cellular blebbing**
- 3D light sheet imaging of cell surface dynamics during macro-pinocytosis & new computational tools

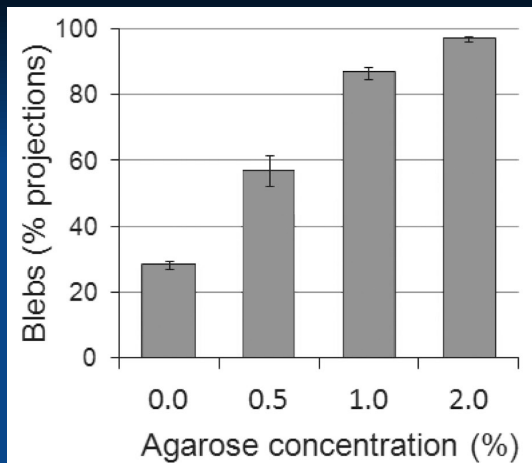
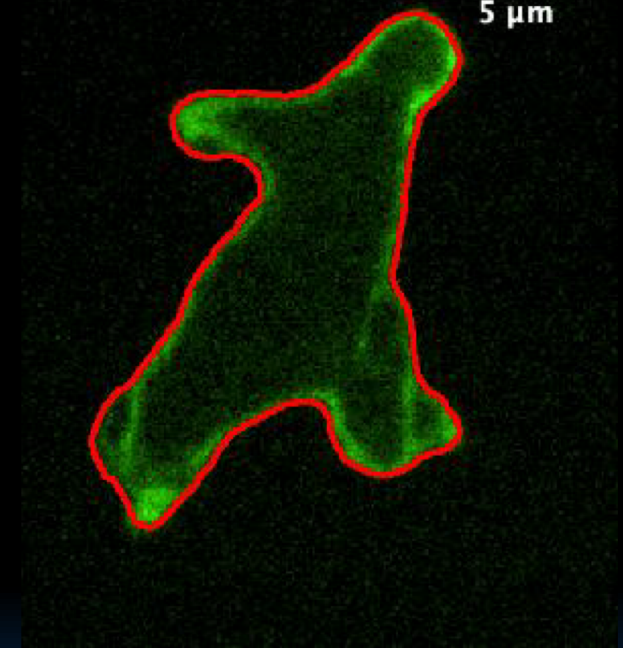
Modelling mechanical aspects of cell motility

Migration under agarose induces blebbing in Dictyostelium

with Evgeny Zatulovskiy, Rob Kay
(MRC LMB, Cambridge)



0.00 sec



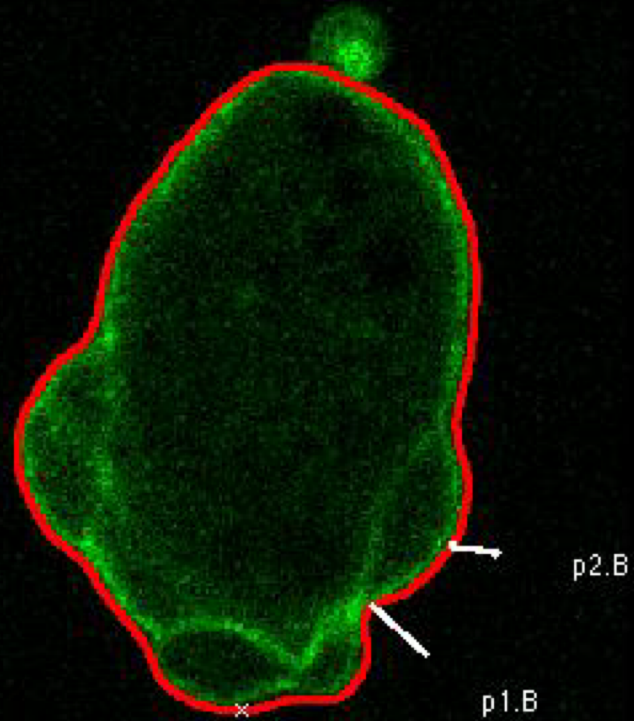
F-actin marker: GFP-ABD (ABP-120)

Spinning disk microscopy (4.5-10 fps)

Confocal microscopy (2 fps)

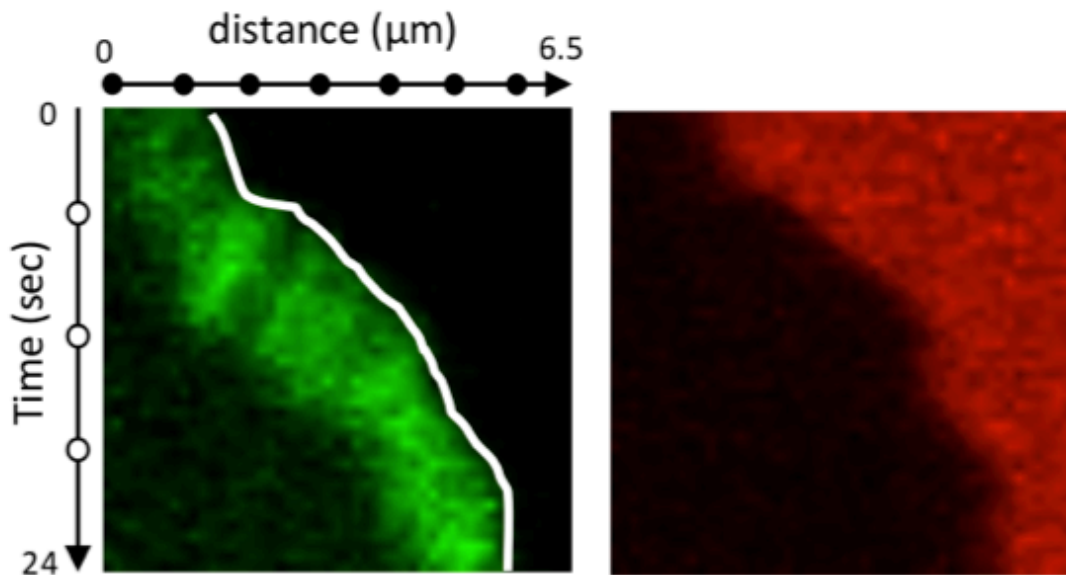
Blebbing only mode (2% agarose), round cells

0.0 sec



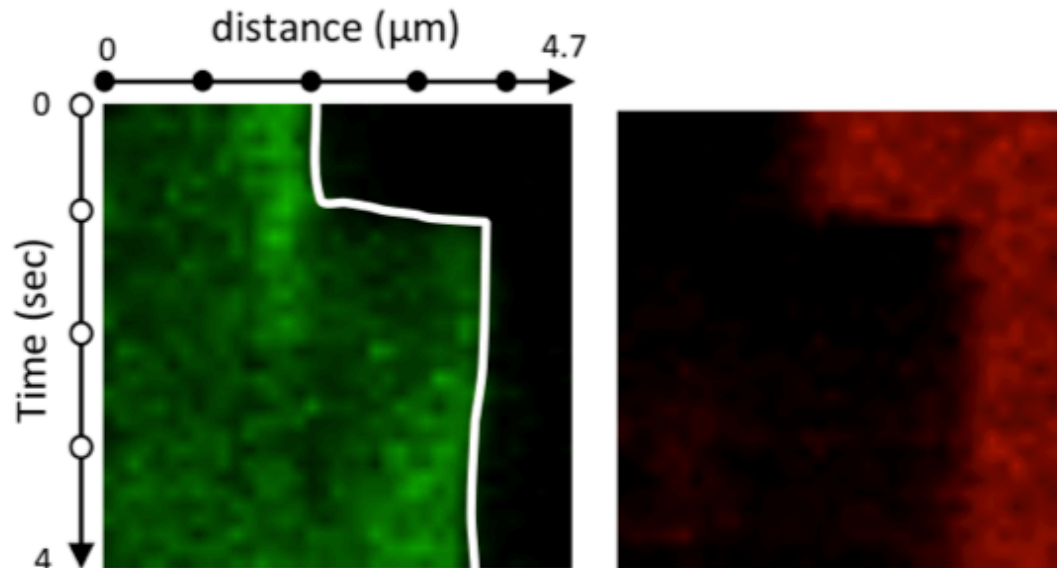
Actin / membrane association in protrusions vs blebs

Actin driven protrusion



Red: Rhodamine Dextran
Green: GFP-ABD

bleb



- Blebbing Myosin-II dependent.
- Myosin-II-null cells can migrate on a 2D surface, but not under agar

Cellular blebbing

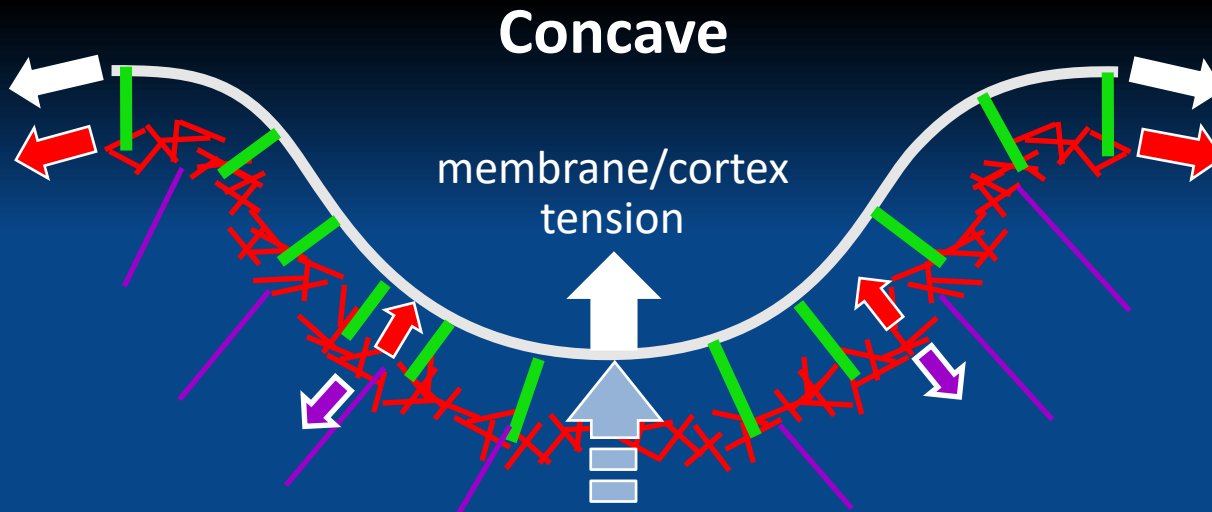
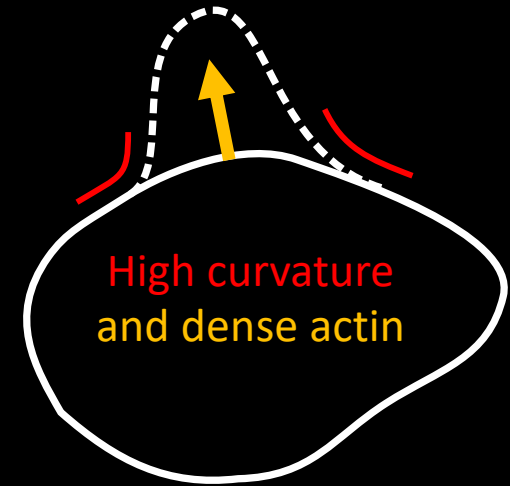
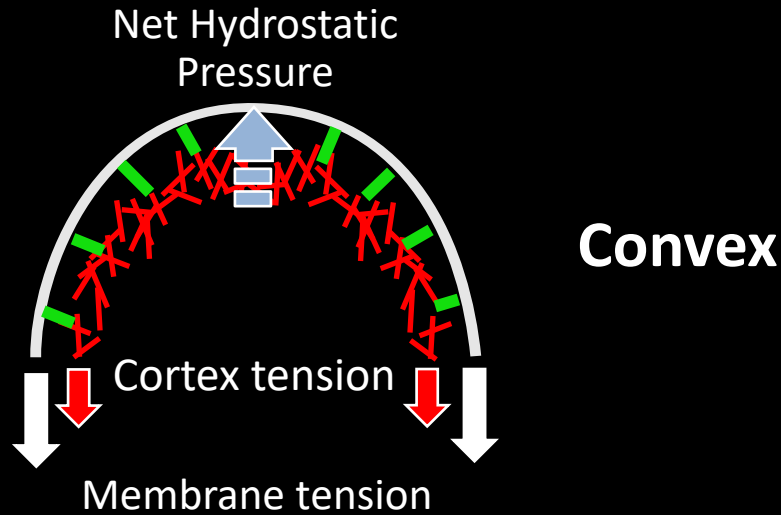
- Myosin-II dependent, driven by hydrostatic pressure
- Often found in cells moving in 3D constrained environments (zebrafish primordial germ cells, tumor cell migration)

How can cells direct blebs to the cell front? How do blebs and actin based protrusions interact?

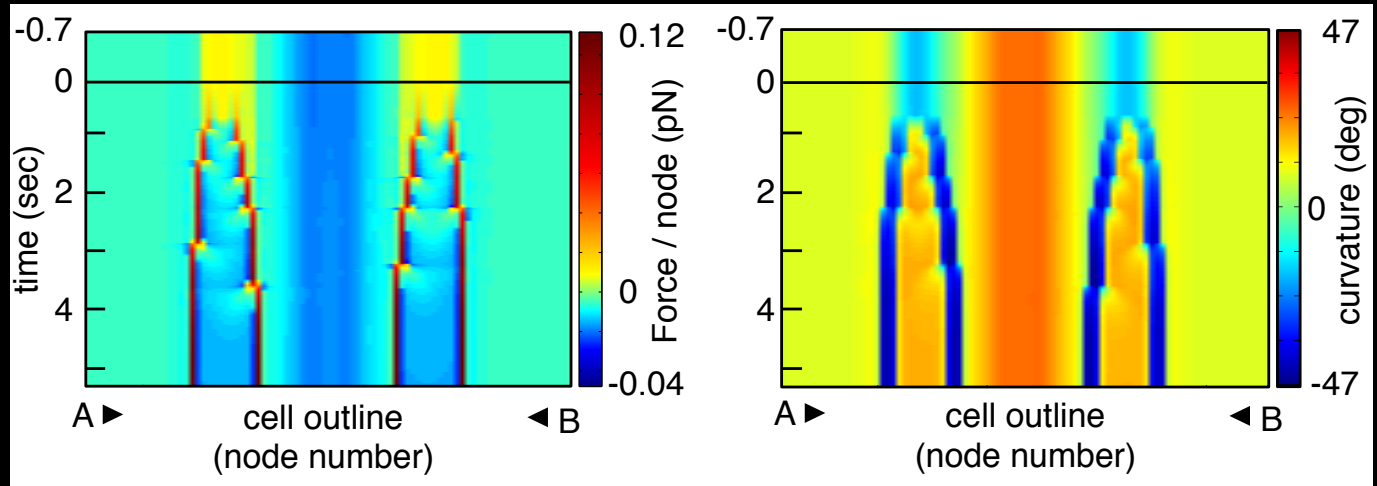
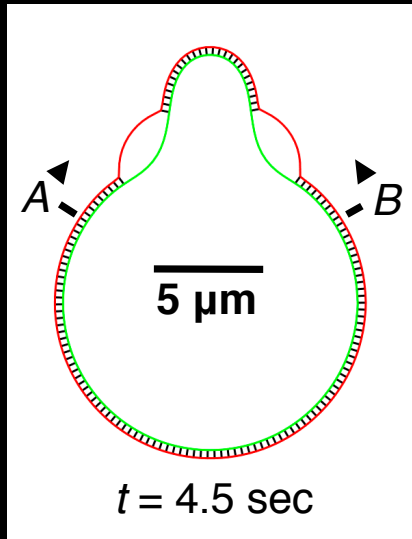
- Previously known regulators of bleb site selection: Weakening of the acto-myosin cortex, local contraction of myosin-II, asymmetric distribution of membrane-cortex linkers
- New: Cell geometry and membrane tension are important factors in bleb site selection, too

Actin driven protrusions can localize blebs through induction of negative curvature

F-actin can drive the formation of blebs by inducing curvature



Towards a predictive model for bleb initiation



Actin cortex is considered fixed during blebbing.

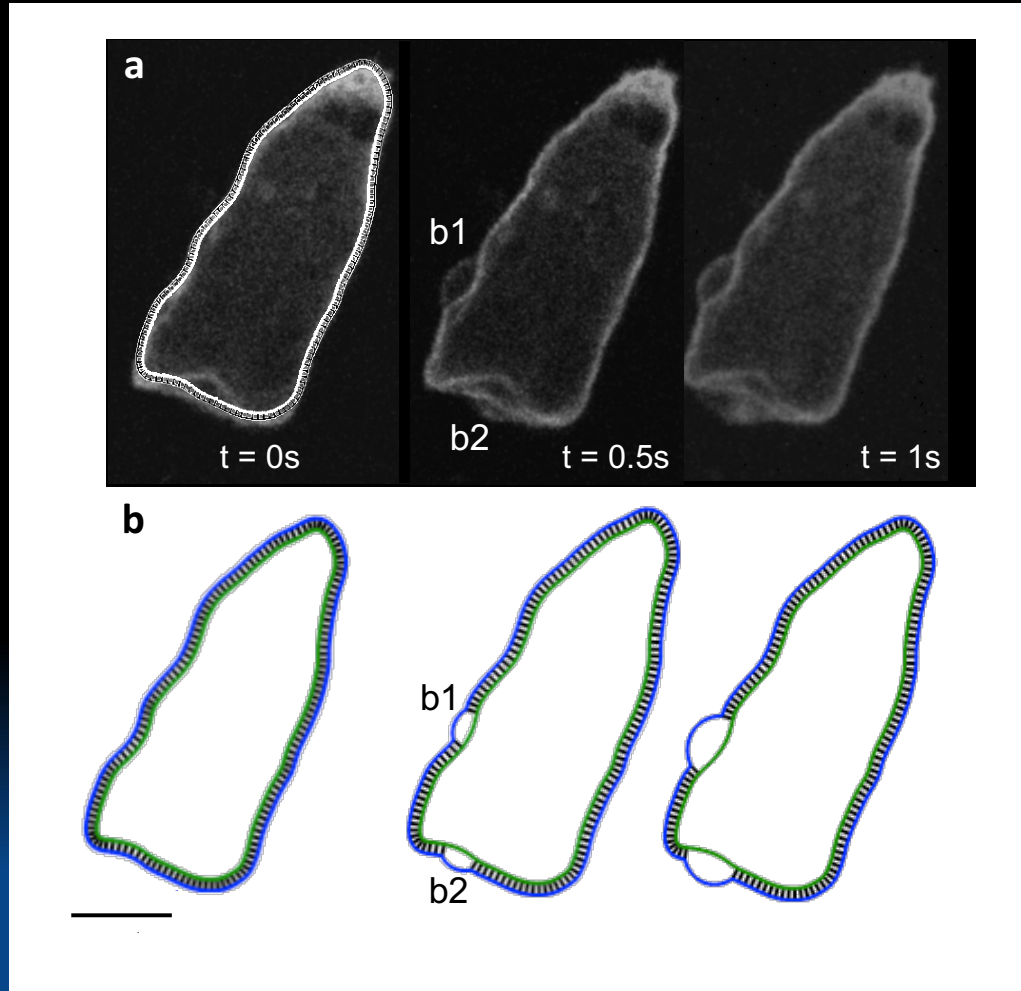
Membrane energy (modified Helfrich model)

$$E_{\text{membrane}} = \oint_0^1 (E_{\text{tension}} + E_{\text{bending}} + E_{\text{coupling}} + E_{\text{pressure}}) ds$$

$$E_{\text{membrane}} = \oint_0^1 \left(\frac{1}{2} \alpha \left(\left| \frac{dx}{ds} \right| - x_0 \right)^2 + \frac{1}{2} \beta \left(\frac{d^2x}{ds^2} \right)^2 + \frac{1}{2} k (L - L_0)^2 + \Delta p \right) ds$$

Linkers break above a certain length.

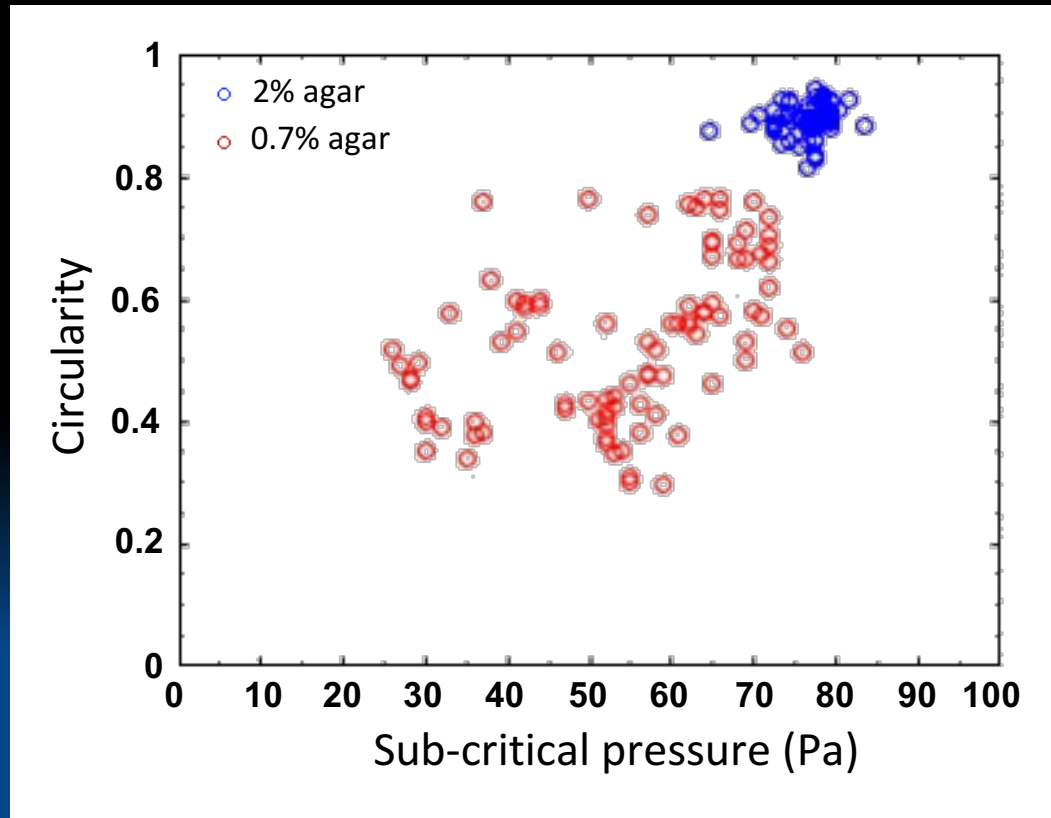
Predicting bleb sites using real cell contours as input



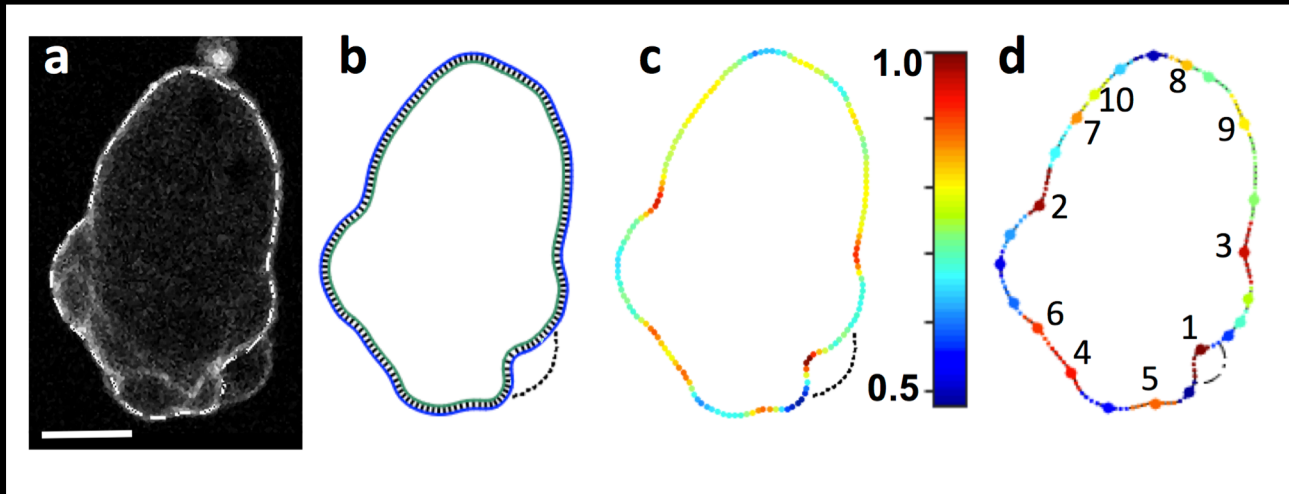
Parameterising subcritical pressure (limit of pressure in the model at which no blebs occur)

- **Subcritical pressure correlates with cell shape**

0.7% agarose: cells elongated; 2%: cells round

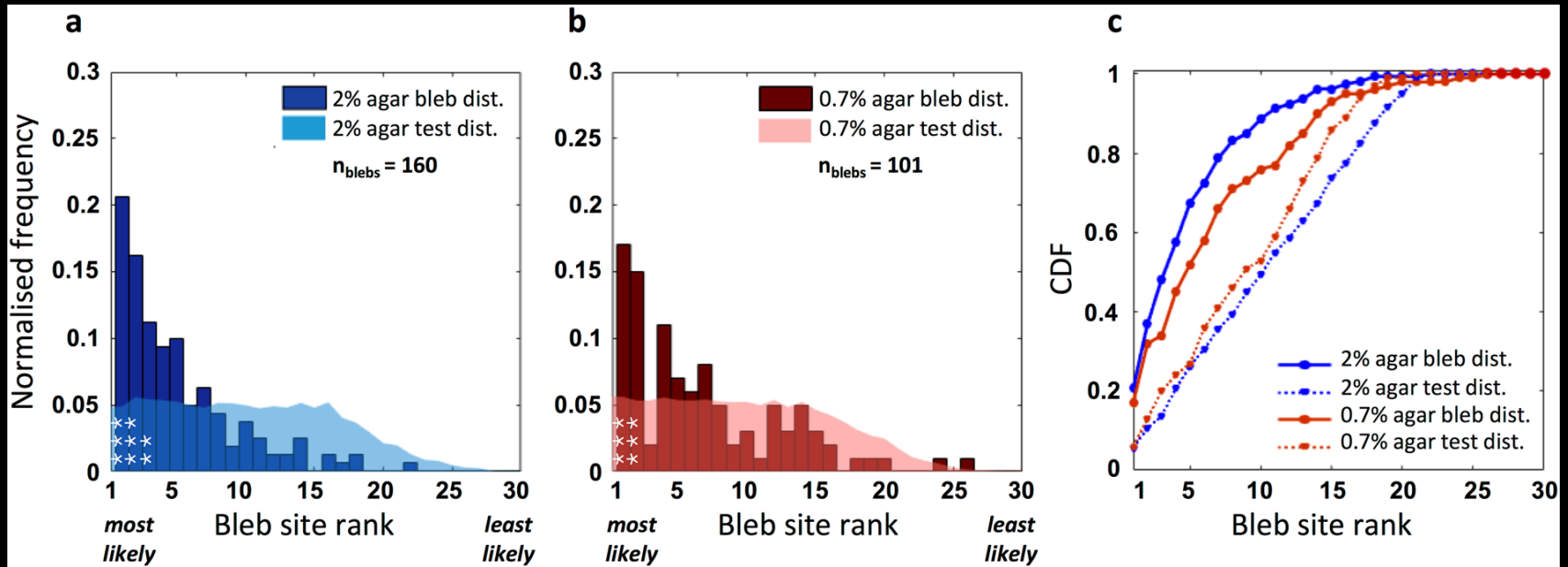


Defining a measure for blebbing propensity:



- Initialize model with real cell contour (a,b)
- Set pressure to sub-critical (highest pressure that does not result in linkers breaking)
- Use linker length at sub-critical pressure as a gauge for blebbing likelihood (c)
- Determine local maxima, and order bleb sites according to their likelihood (d)

Frequency of experimentally observed blebs plotted against model bleb site rank



- Distributions are strongly weighted towards the most likely ranked sites predicted by the model
- Cumulative distribution function: under-curve areas of 82% (2% agarose) and 76% (0.7% agarose) show that the original model predicts bleb site selection in a highly resistive environment better

Summary blebbing model

- Under high mechanical resistance (round cells, highly pressurised), mechanical forces seem to play the dominant role
- Under low mechanical resistance (elongated cells) the model supports the hypothesis that gradients in cortex-membrane linker strength play an additional role (Talin in *Dictyostelium*)
- Because we deal with a physical system, the same principles can be generalised to other cell types (fish)

Outline

- Analysing dynamic fluorescence distributions in the cortex of moving cells (QuimP software)
- Parameterization of different models for cell reorientation
- The role of membrane tension in cellular blebbing
- **3D light sheet imaging of cell surface dynamics during macro-pinocytosis & new computational tools**

Actin driven surface dynamics during macropinocytosis: Cell drinking

joint project with Rob Kay, Peggy Paschke, MRC LMB, Cambridge

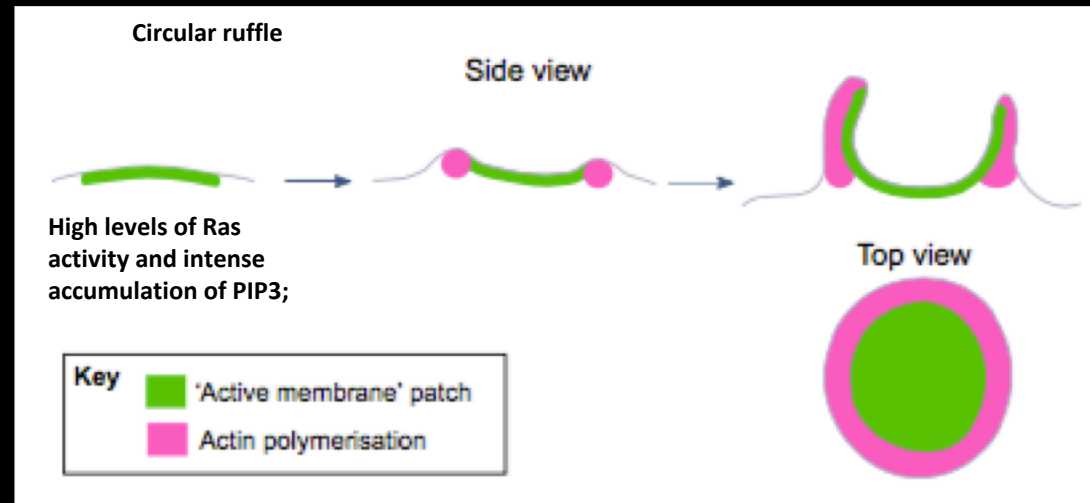
Important in

- sampling of antigens by immune cells
- meeting the high energy demands of cancer cells
- the uptake of large viruses like Ebola

Our interests

- Macropinosome evolution
- Mechanics of cup closure

Organisation of cup-like structures



Bloomfield G. and Kay R., 2016. *J. Cell Sci.* **129**: : 2697-2705

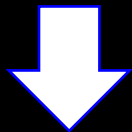
Motivation for imaging in 3D

– Easy to misinterpret 2D data

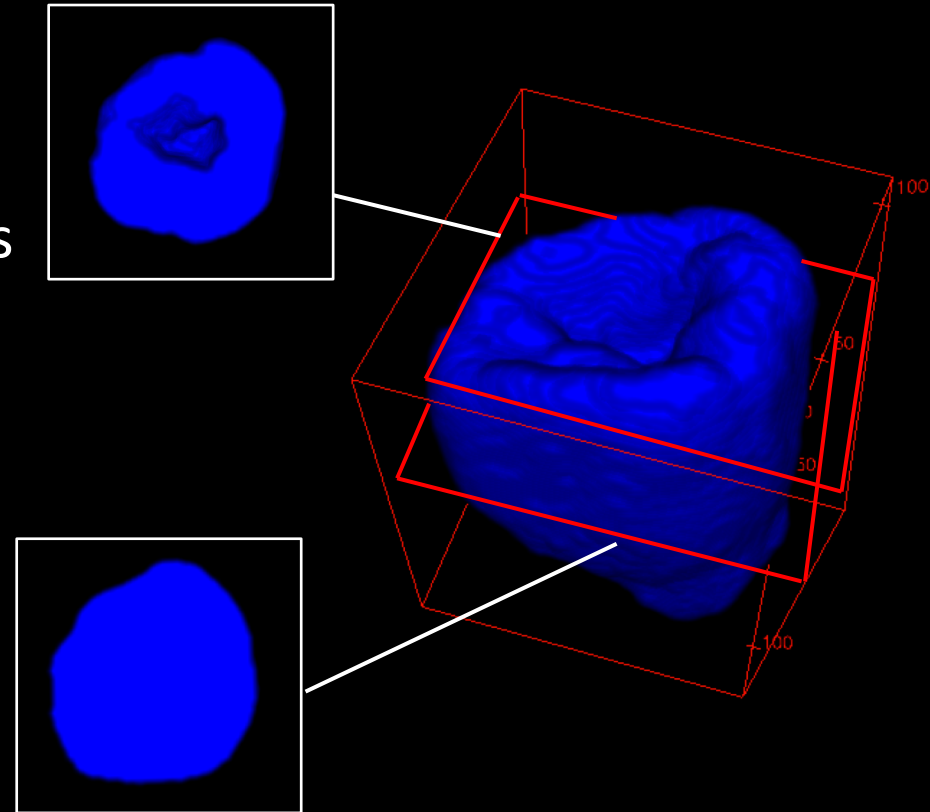
AIM: to create a data pipeline for processing and analysing 3D images

Challenges for Dictyostelium data:

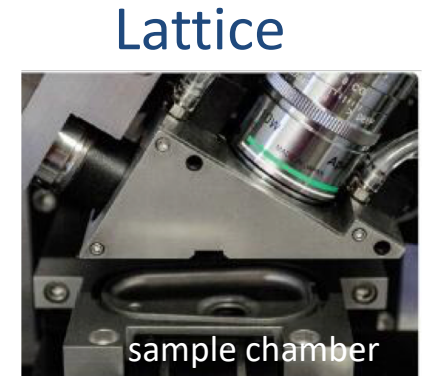
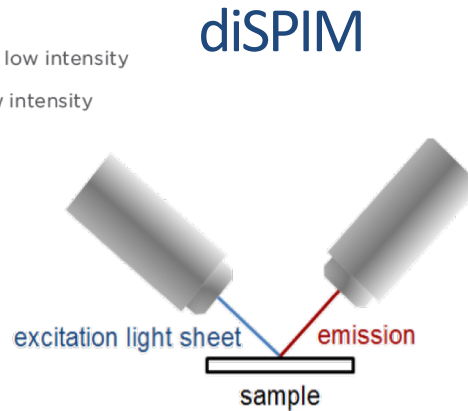
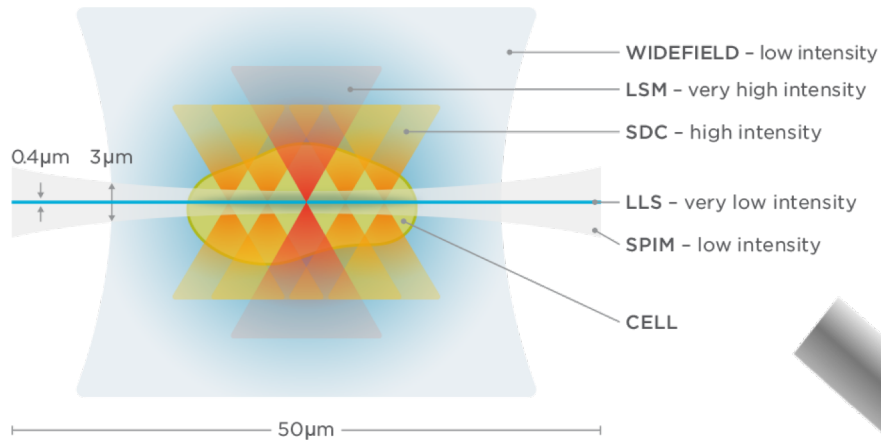
- Phototoxicity
- Speed



Light sheet microscopy

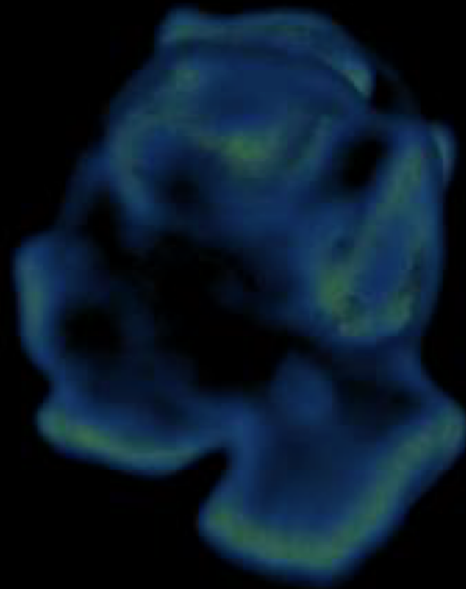


3D single cell light sheet imaging offers ultra low phototoxicity

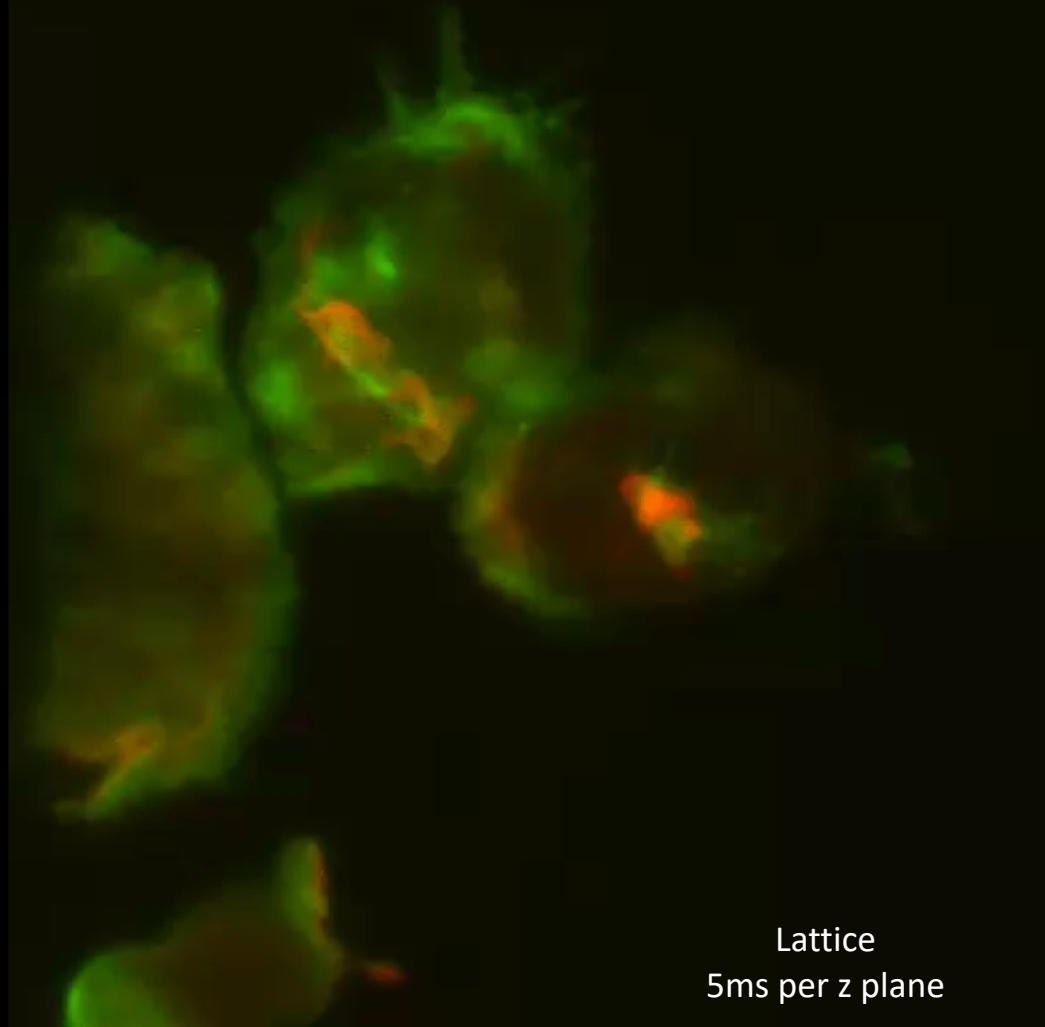


Number of objectives	2	1
Scan type	Objectives moved by piezos	Stage moved by piezos
Sheet thickness	4µm at 50µm length	0.4µm at 50µm length
Sample setup	Standard 10ml culture plate	5mm coverslip
Minimum exposure possible	1ms	3ms
Minimum z step size	0.2µm	0.1µm
Magnification	40X	62.5X
Maximum exposure for fusion deconvolution	10ms	--

Example data: F-actin label

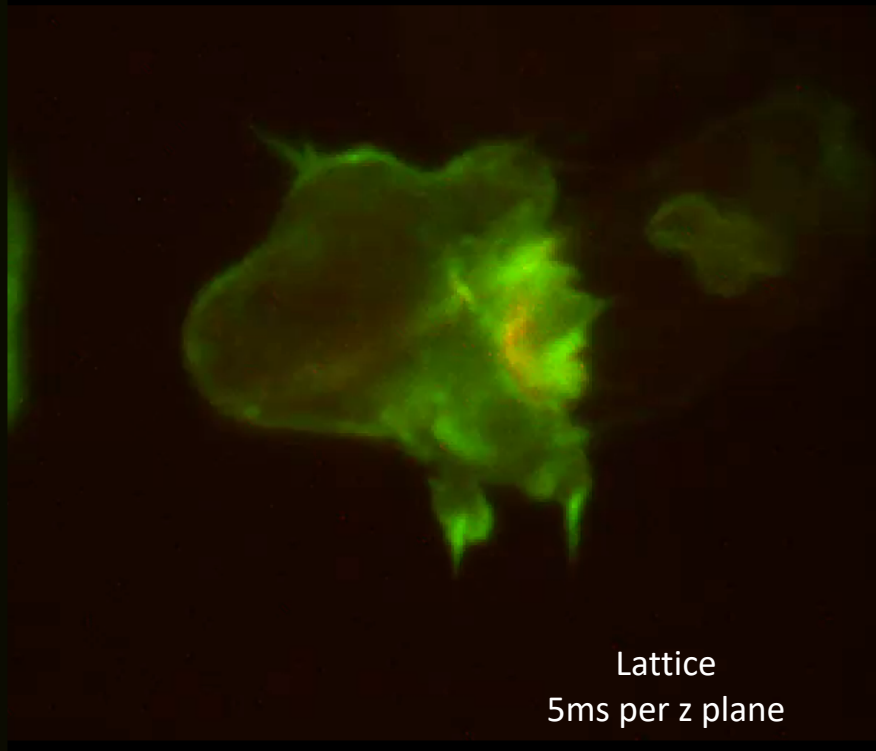


Dual-colour rapid 3D imaging

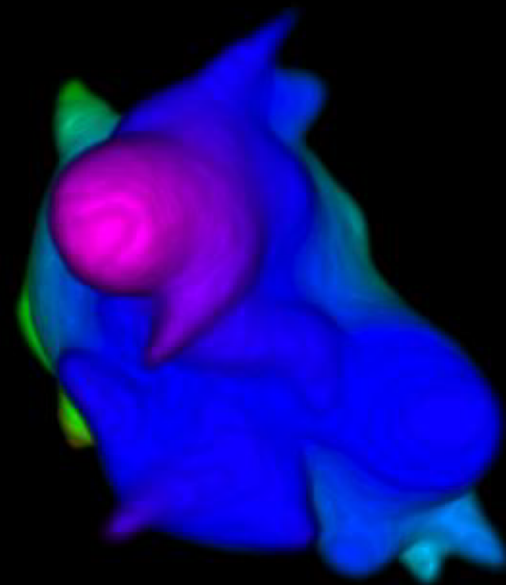
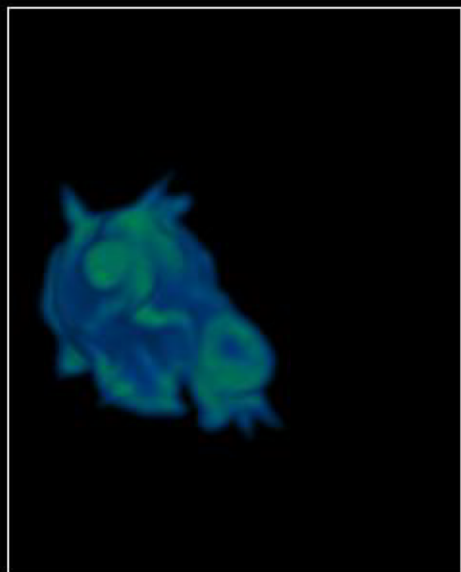


F-actin and PIP3

maximum projection movies

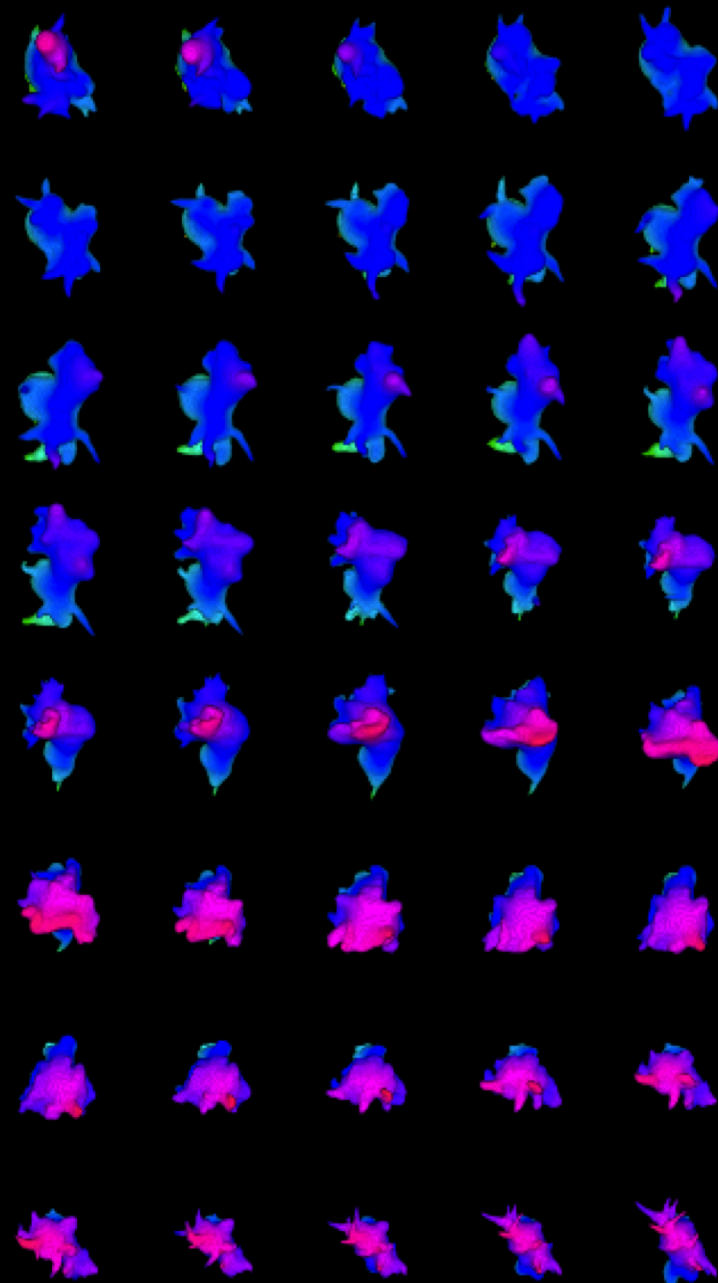


Full time series reconstruction (WEKA)



Colour: depth
Purple front
Green rear

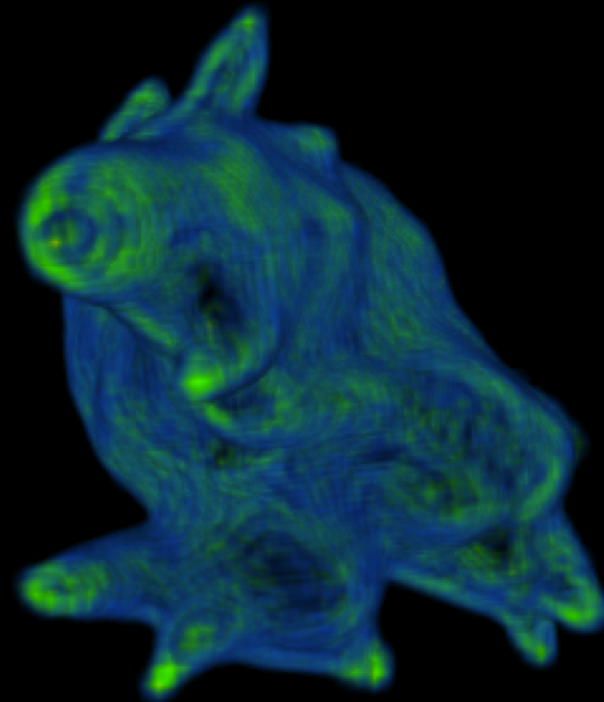
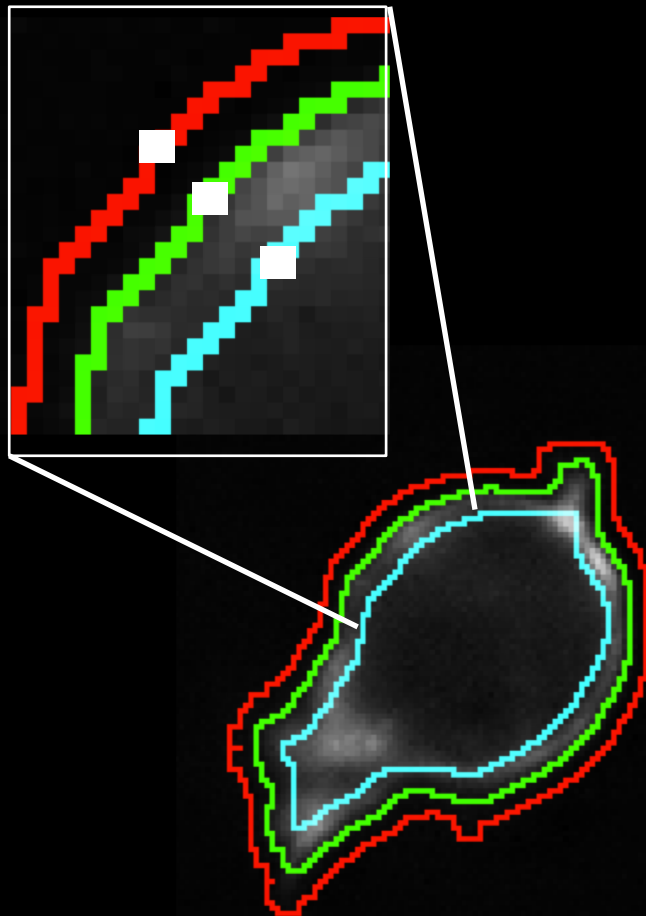
0.00 s



Mapping cortical fluorescence onto cell surfaces

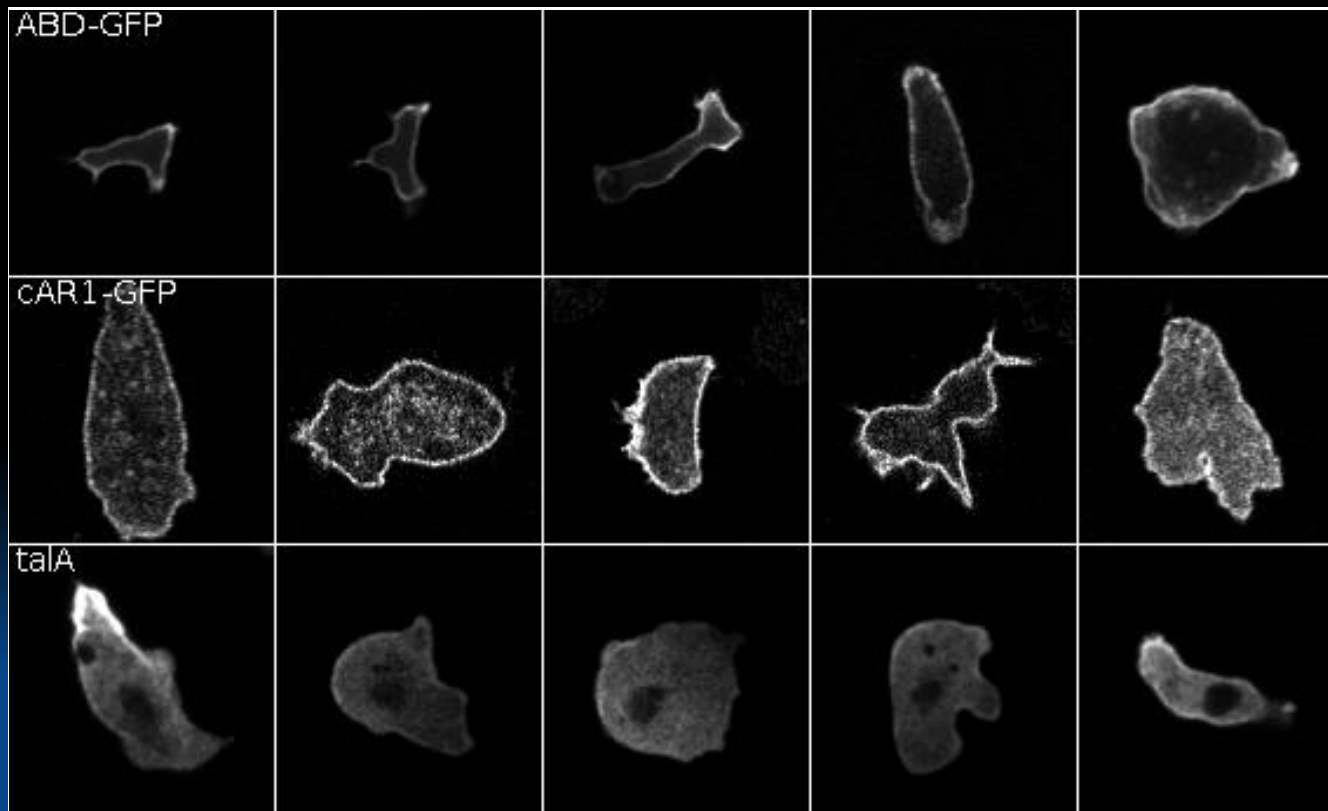
Goal:

- Map the different stages of macropinosome evolution
- Correlate fluorescence with shape deformations and infer forces acting on the membrane



GENERATIVE ADVERSARIAL NETWORKS FOR AUGMENTING TRAINING DATA OF MICROSCOPIC CELL IMAGES

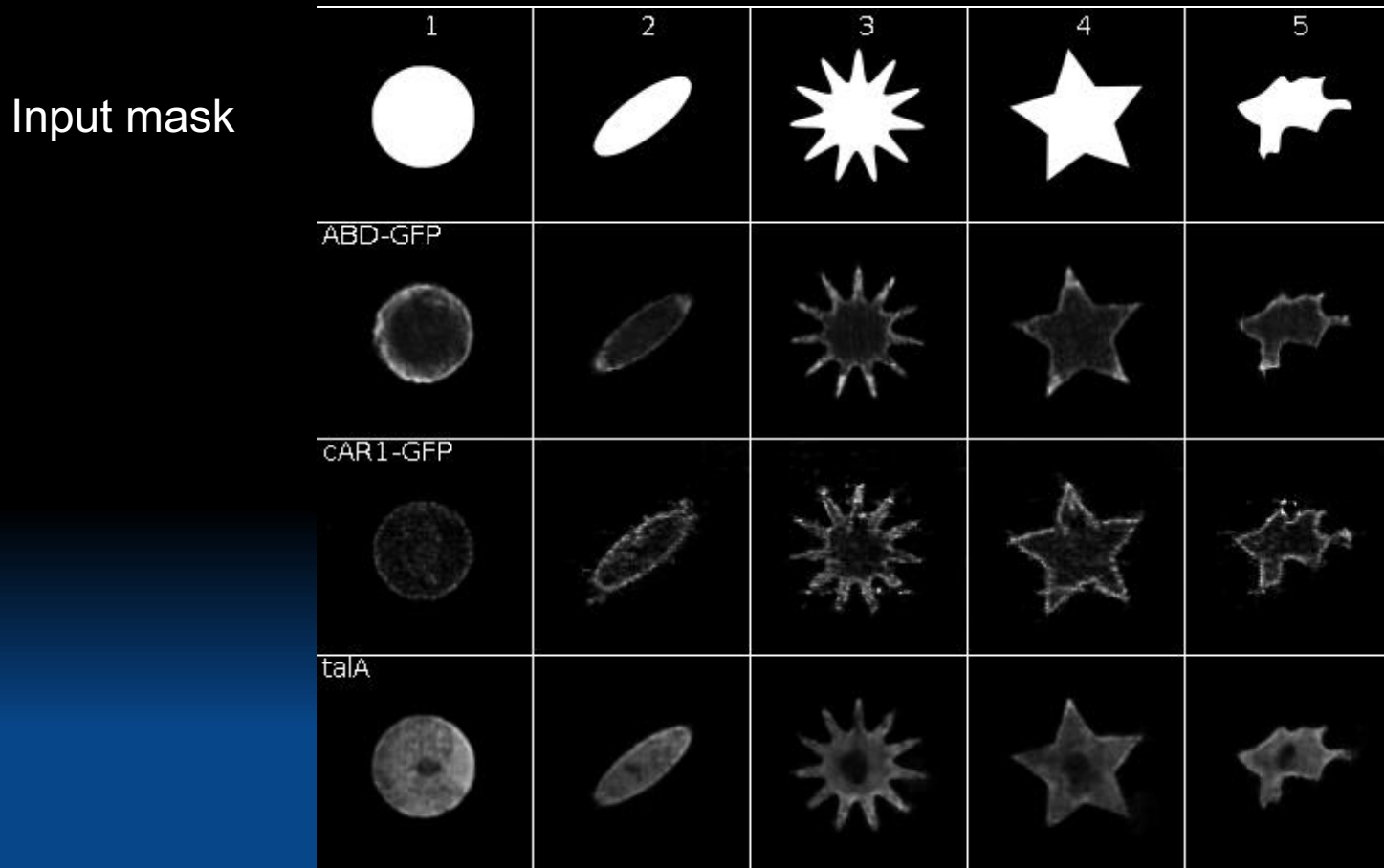
- How can we validate methods for 3D segmentation if manual validation of 3D training data is prohibitive?



Original data, three different biological labels

Generating synthetic cell images trained from specific labels, using arbitrary shapes

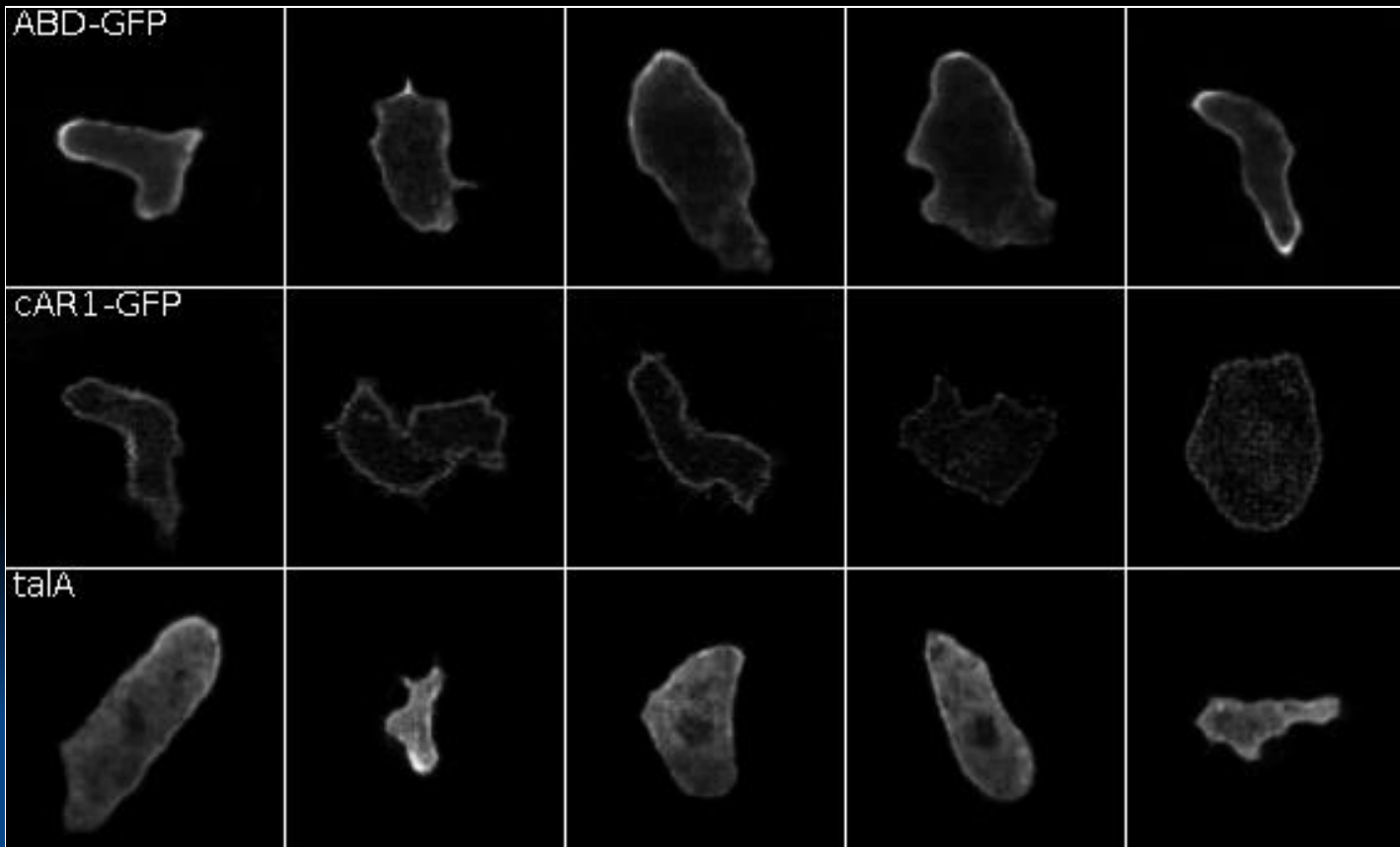
- The network reproduces the main characteristic features of different label distributions, including noise.



P. Isola, J.-Y. Zhu, T. Zhou, and A.A. Efros, "Image-to-Image Translation with Conditional Adversarial Networks," in *Proc. CVPR*, 2017, pp. 1125–1134.

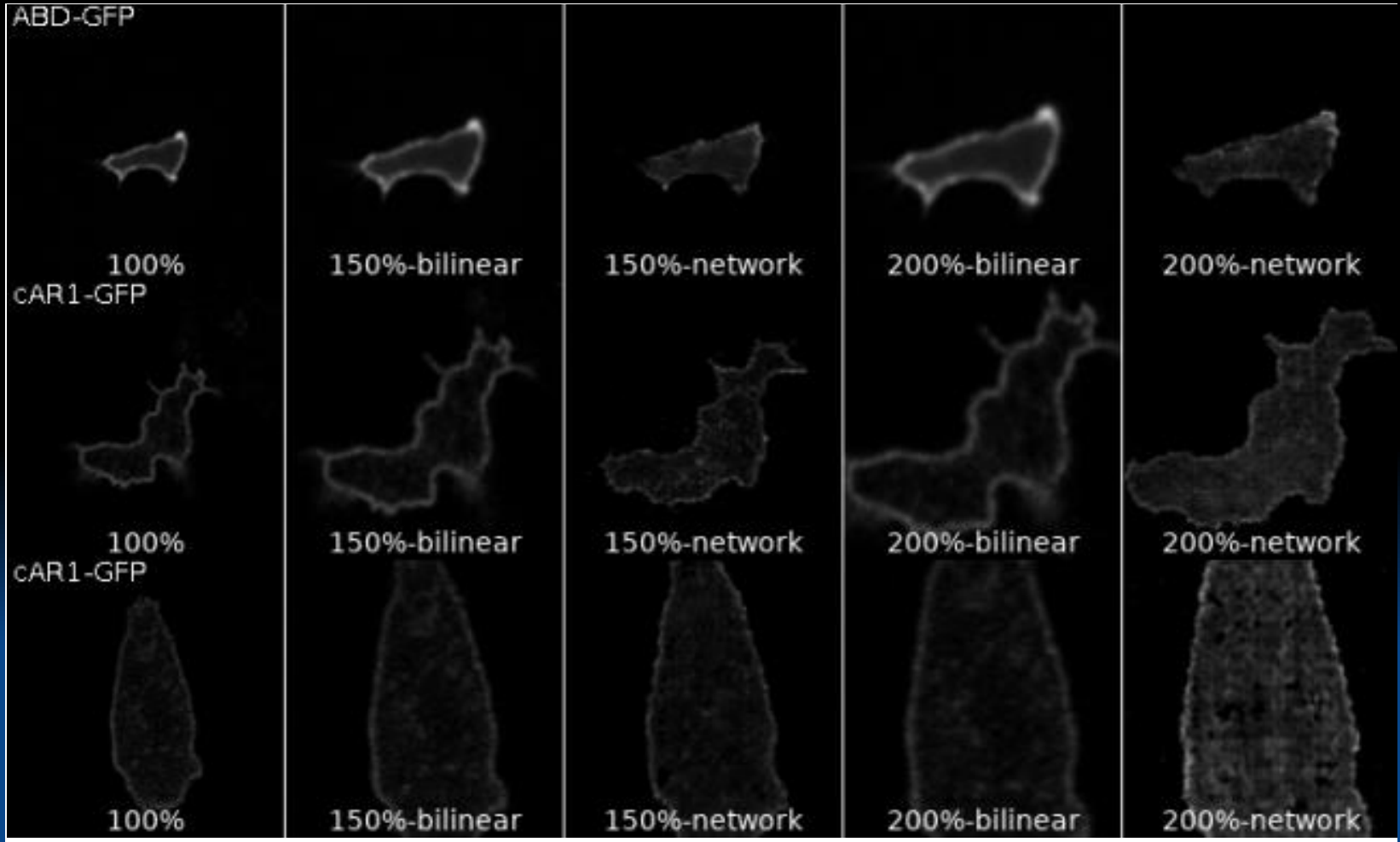
Generating synthetic cell images, using real cell shapes

- Validating how realistic the output is, is very difficult. So far biological experts in the field seem to be impressed...



GANs allow to produce more realistic augmented data

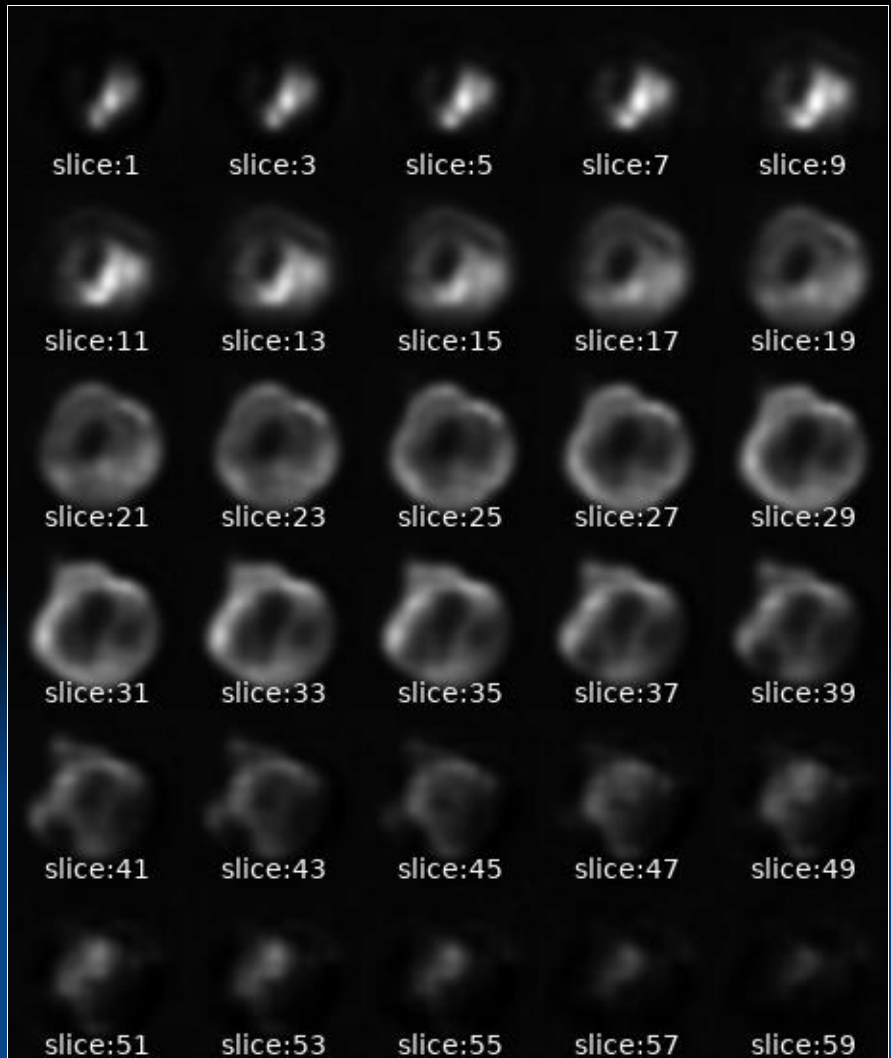
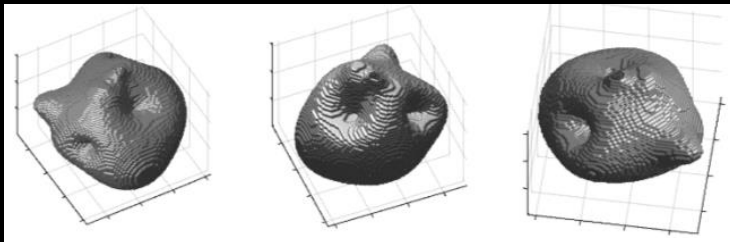
- When scaling input shapes, synthetic labelling preserves the original length scale (resolution) of features, and retains the inherent noise characteristics



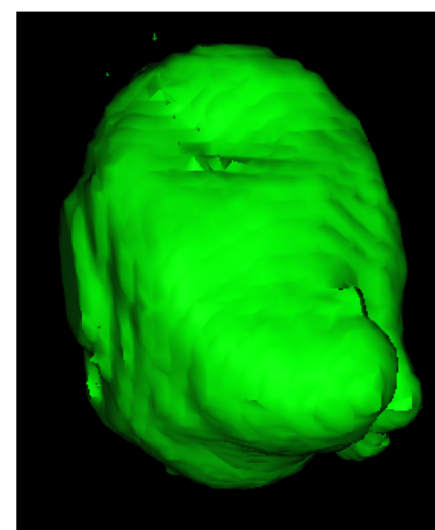
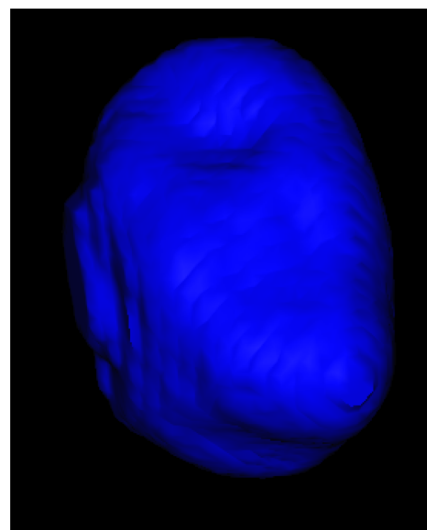
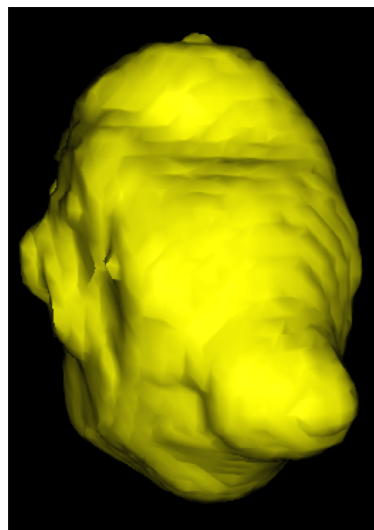
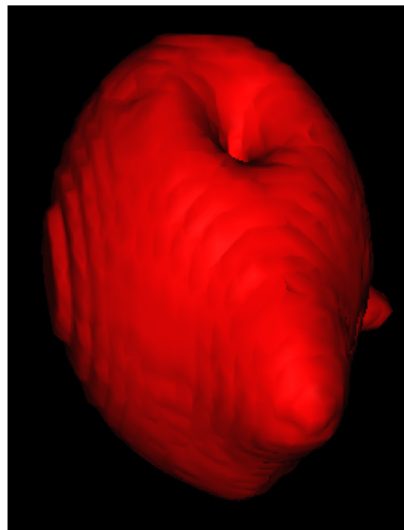
Synthetic 3D data

- Obtaining ground truth data for 3D data sets is almost impossible. Synthetic data holds great promise for validating different methods, and augmenting training data sets

Artificial input mask



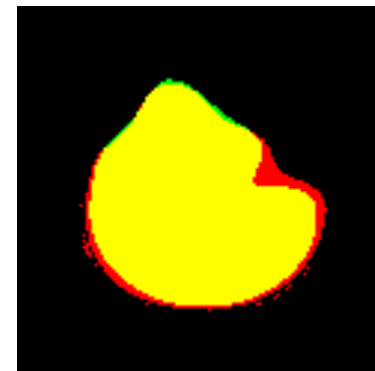
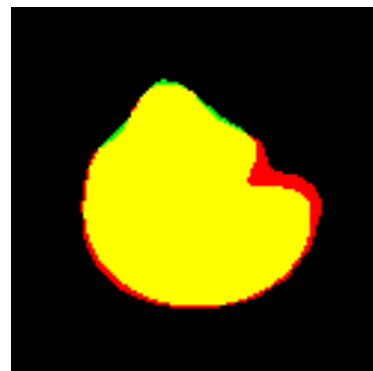
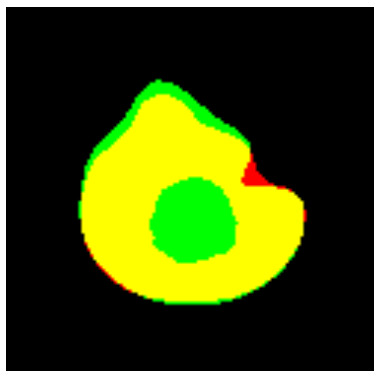
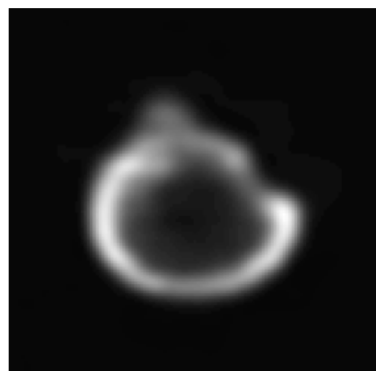
Segmentation of synthetic data with known ground truth



Otsu

RW

WEKA



Summary 3D imaging & computational tools

- Light sheet microscopy enables us to resolve fast cellular processes in unprecedented detail
- GANs are a very promising tool for realistic data augmentation and creating “synthetic ground truth data”

Acknowledgements

Current



Sharon Collier: Models / experiments on Blebbing and Macropinocytosis / Light sheet microscopy



Piotr Baniukiewicz: QuimP development



Josiah Lutton: Mapping 3D cell surface dynamics

Alumni



Richard Tyson, Early QuimP, Blebbing in *Dictyostelium*



Chengjin Du, CellTracker: Quantifying transcription factor dynamics, 3D cell reconstructions



Robert Lockley: Modelling cell polarity

Main Collaborators

Rob Kay, MRC-LMB, Cambridge

Andrew McAinsh, Warwick

Graham Ladds, Warwick, now Cambridge

Kees Weijer, University of Dundee

Len Stephens, Babraham, Cambridge; Mike White, Manchester